ROBERT R. McCORMICK SCHOOL OF ENGINEERING AND APPLIED SCIENCE

# Probing Molecular Electronics with Scanning Probe Microscopy

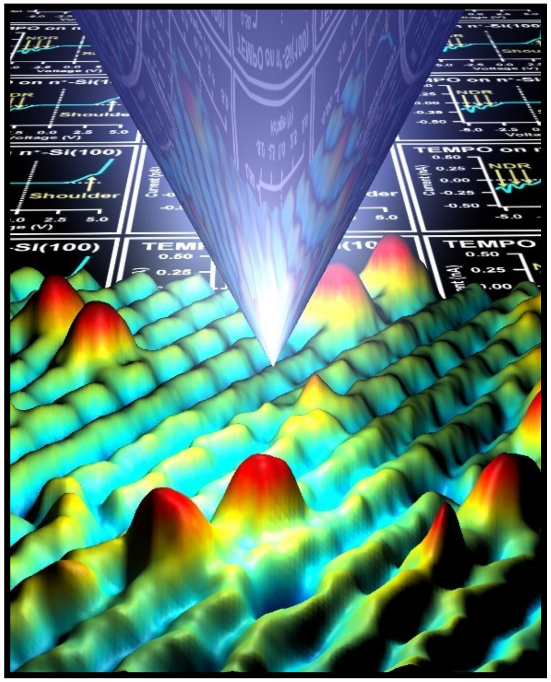

**Mark C. Hersam**
**Assistant Professor**

Department of Materials Science and Engineering,
Northwestern University, Evanston, IL 60208-3108
Ph: 847-491-2696, m-hersam@northwestern.edu
WWW: http://www.hersam-group.northwestern.edu/

# Outline

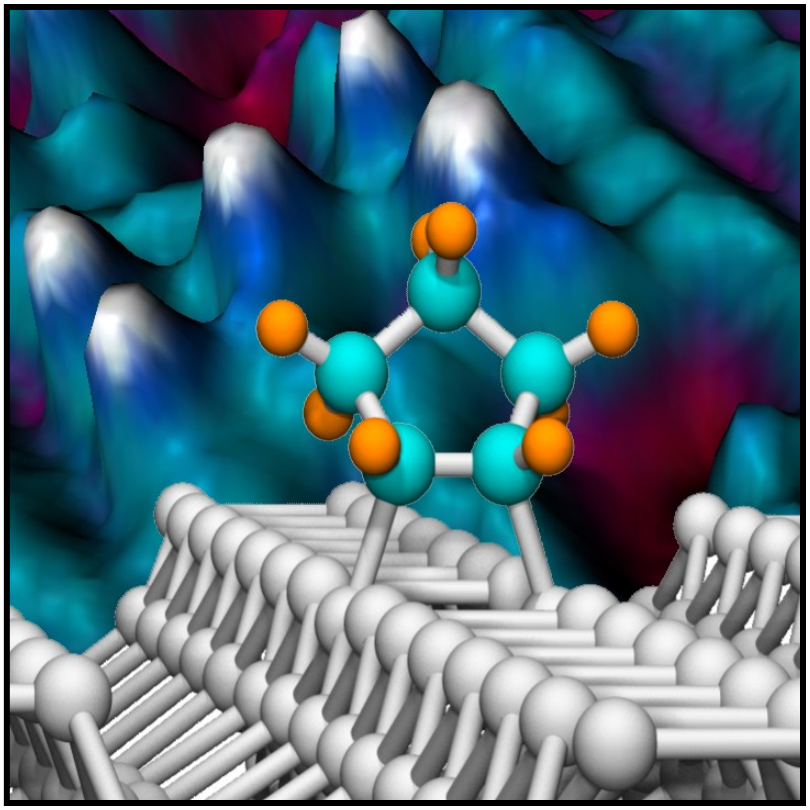

- Motivation
- Background
- Construction
- SPM Techniques

# An Ideal Experiment for Probing Molecular Conduction

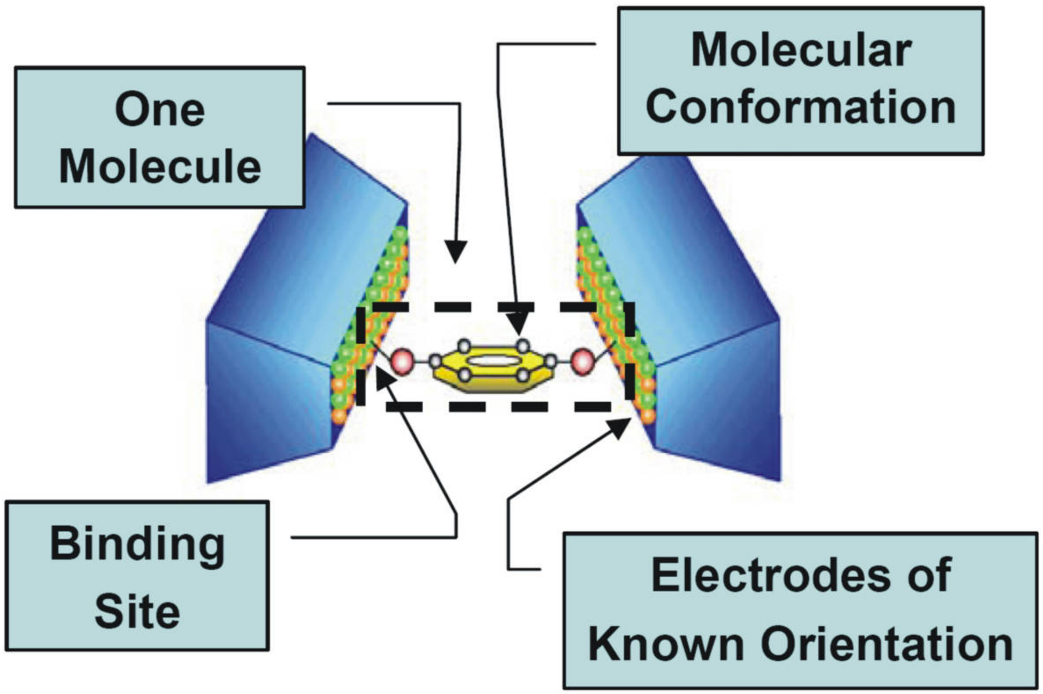

One Molecule

Molecular Conformation

Binding Site

Electrodes of Known Orientation

M. C. Hersam, *et al.*, *MRS Bulletin*, **29**, 385 (2004).

# Real Experimental Strategies for Probing Molecular Conduction

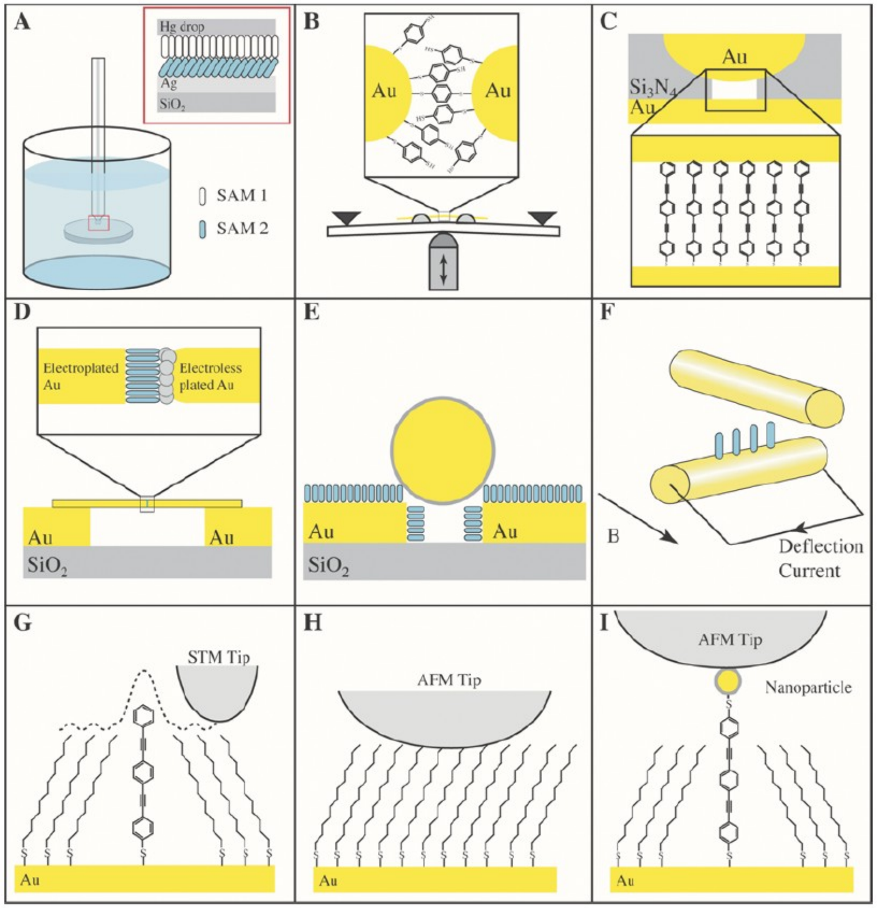

B. A. Mantooth, *et al.*,
*Proc. IEEE*, **91**, 1785 (2003).

# The Origin of Scanning Probe Microscopy

C. Julian Chen, *Introduction to Scanning Tunneling Microscopy*

# The Scanning Tunneling Microscope

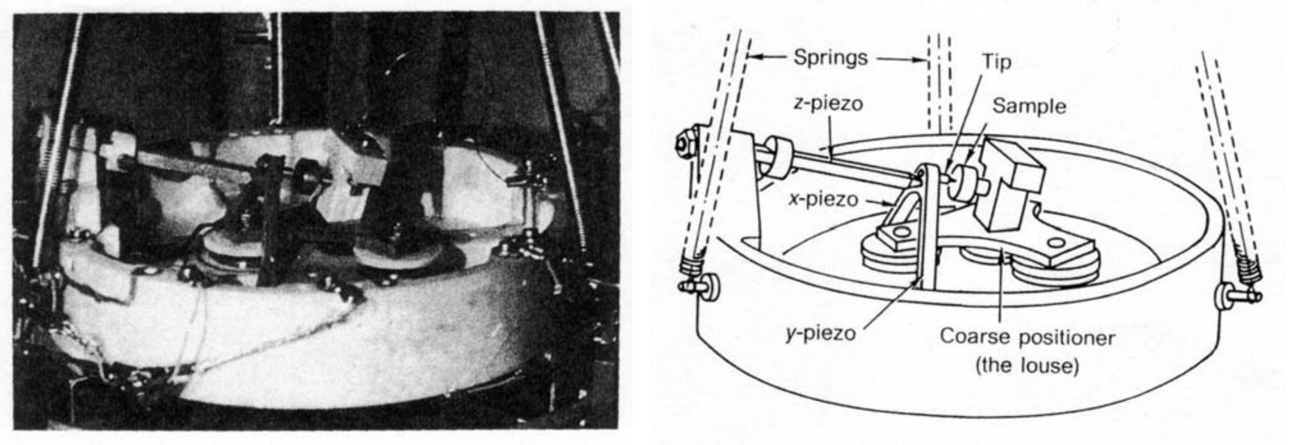

**Plate 2. A humble gadget that shocked the science community.** Upper, a photograph of an earlier version of the scanning tunneling microscope that enabled real-space imaging of the Si(111)-7×7 structure. Lower, a schematic of it. See Binnig and Rohrer (1982). Original photograph courtesy of Ch. Gerber.

- STM invented by Gerd Binnig and Heinrich Rohrer in 1982
- Led to Nobel Prize in Physics, 1986

C. Julian Chen, *Introduction to Scanning Tunneling Microscopy*

# Si(111)-7×7: “Stairway to Heaven”

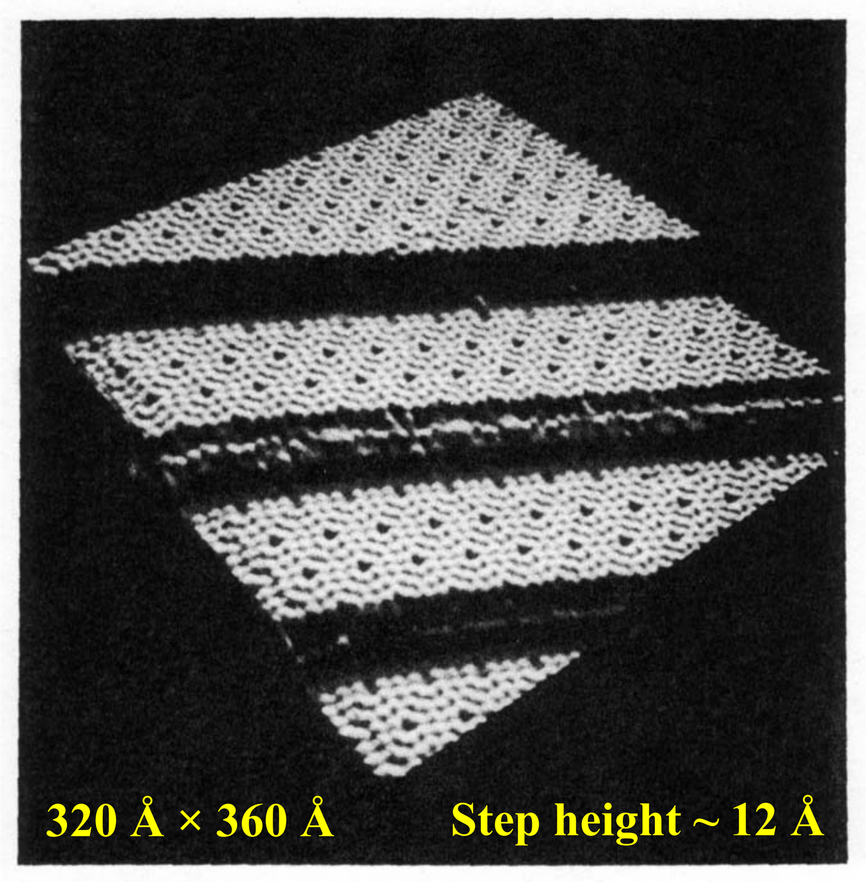

C. Julian Chen, *Introduction to Scanning Tunneling Microscopy*

# Scanning Tunneling Microscope Schematic

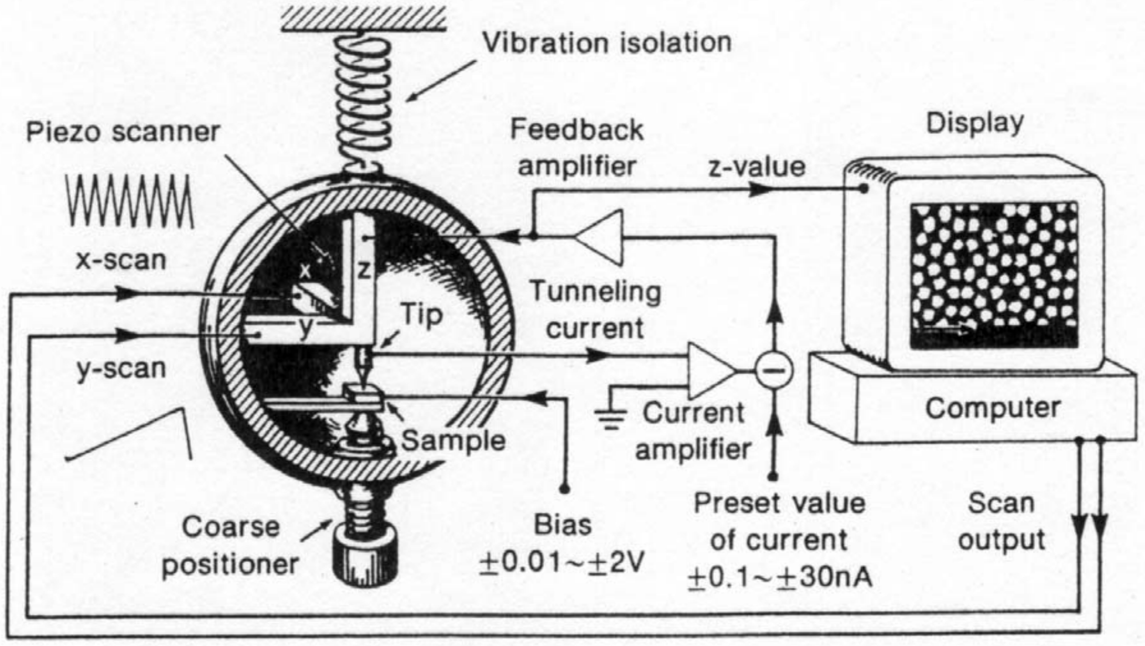

Fig. 1.1. Schematic diagram of the scanning tunneling microscope.

C. Julian Chen, *Introduction to Scanning Tunneling Microscopy*

# One-Dimensional Tunnel Junction

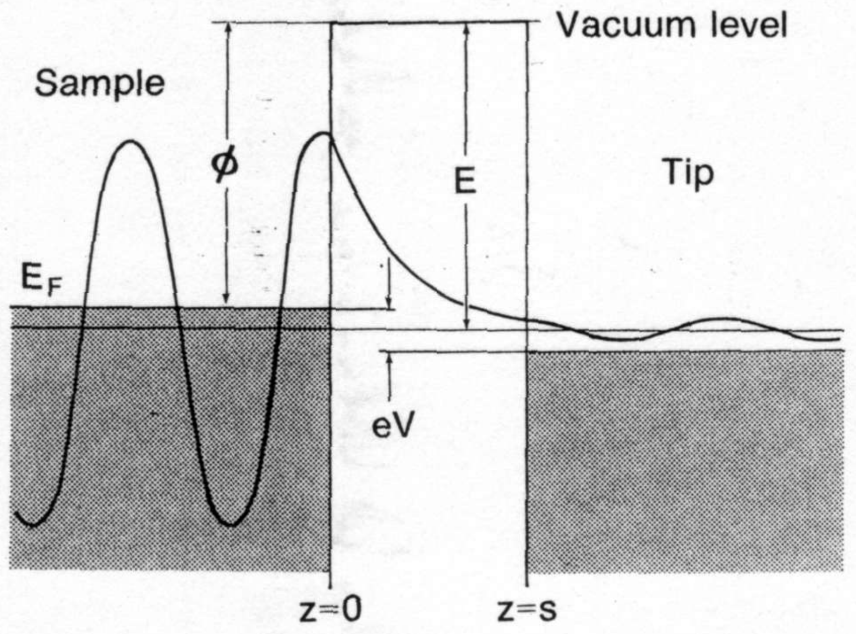

**Fig. 1.4. A one-dimensional metal–vacuum–metal tunneling junction**. The sample, left, and the tip, right, are modeled as semi-infinite pieces of free-electron metal.

C. Julian Chen, *Introduction to Scanning Tunneling Microscopy*

# Tunneling Current – Approach #1

Assume metal-vacuum-metal junction, solve Schrödinger Equation:

$$I \propto V\rho_s e^{-2kW}, \text{ where } k = \frac{\sqrt{2m\phi}}{\hbar} = 0.51\sqrt{\varphi(eV)}\ \text{Å}^{-1}$$

$I$ = tunneling current

$V$ = tip-sample voltage

$\rho_s$ = local density of states of sample

$W$ = width of barrier

Typically, $\varphi \sim 4$ eV → $k \sim 1$ Å$^{-1}$

→ Current decays by $e^2 \sim 7.4$ times per Å

# Bardeen Tunneling Theory

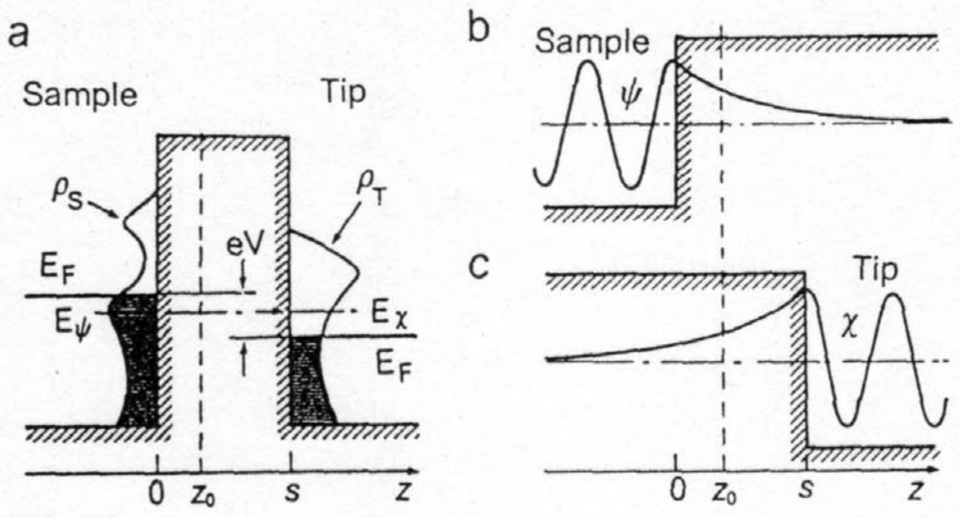

**Fig. 1.20. The Bardeen approach to tunneling theory**. Instead of solving the Schrödinger equation for the coupled system, a, Bardeen (1960) makes clever use of perturbation theory. Starting with two free subsystems, b and c, the tunneling current is calculated through the overlap of the wavefunctions of free systems using the *Fermi golden rule*.

C. Julian Chen, *Introduction to Scanning Tunneling Microscopy*

# Tunneling Current – Approach #2

Consider overlap of wavefunctions from either side of barrier:

Using Fermi's Golden Rule (assuming kT << energy resolution of the measurement),

$$I \propto \int_0^{eV} \overset{\text{sample}}{\rho_s}(E_F - eV + \varepsilon)\,\overset{\text{tip}}{\rho_t}(E_F + \varepsilon)\,d\varepsilon$$

For a free electron metal tip, $\rho_t$ is constant:

$$\frac{dI}{dV} \propto \rho_s(E_F - eV)$$ → STM Spectroscopy

# Atomic Force Microscopy

- Invented at Stanford by Binnig and Quate in 1986
- Bring tip-mounted micromachined cantilever into contact or close proximity of the surface
- “Atomic forces” deflect cantilever and is detected with laser deflection into a position sensitive photodiode
- Cantilever deflection is control signal for the feedback loop
- AFM can be done on “any surface” (i.e., conductive, insulating, semiconducting, biological, etc.) in “any environment” (i.e., air, vacuum, liquid, etc.)

# Atomic Force Microscope Cantilevers

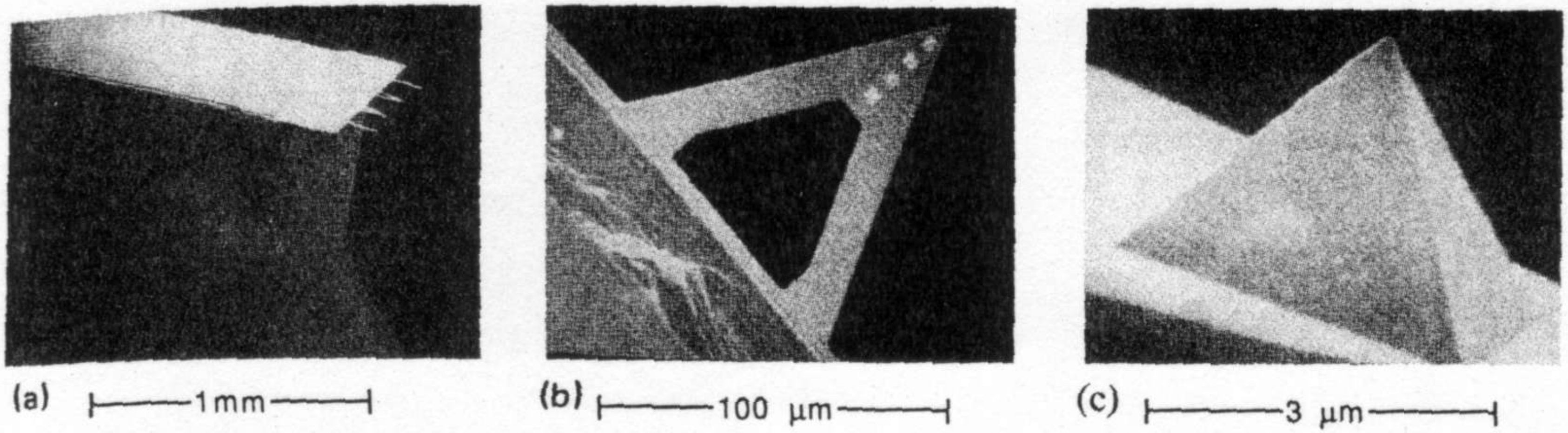

**Fig. 15.3. Microcantilever for atomic-force microscopy.** (a) A glass substrate with four cantilevers. (b) One of the cantilevers. (c) Close-up view of the tip. (After Albrecht et al. 1990.)

C. Julian Chen, *Introduction to Scanning Tunneling Microscopy*

# Force Detection with Optical Beam Deflection

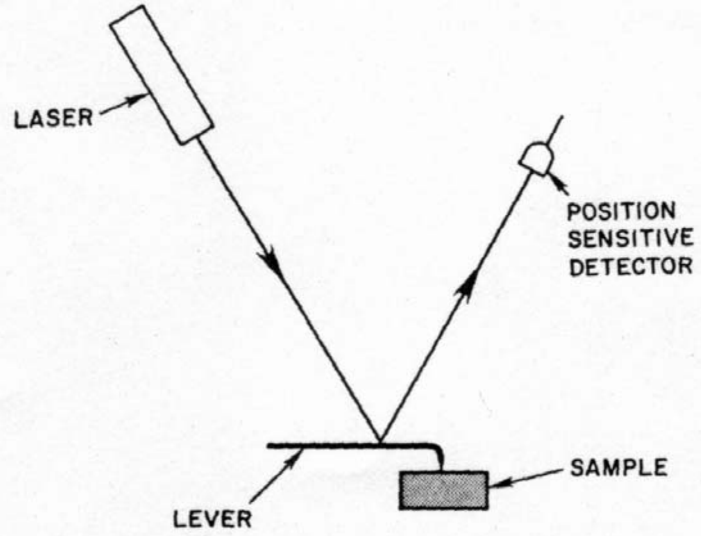

**Fig. 15.7. Detection of cantilever deflection by optical beam deflection.** A light beam, typically from a solid-state laser, is reflected by the top surface of the cantilever. The cantilever is vacuum deposited with gold, which reflects red light almost perfectly. The deflection of the mechanical cantilever deflects the optical beam, thus changing the proportion of light falling on the two halves of the split photodiode. The difference of the signals from the two halves of the photodiode is detected. (Reproduced from Meyer and Amer, 1988, with permission.)

C. Julian Chen, *Introduction to Scanning Tunneling Microscopy*

# Fluid Cell for Atomic Force Microscopy

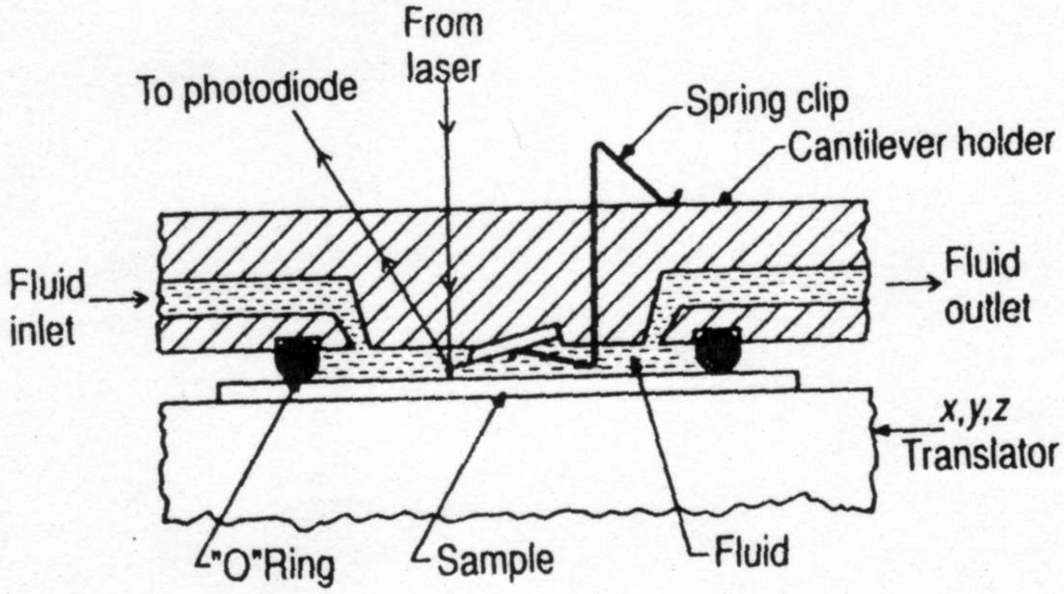

**Fig. 15.10. Fluid cell for AFM study of electrochemistry.** (Reproduced from Manne et al., 1991, with permission.)

C. Julian Chen, *Introduction to Scanning Tunneling Microscopy*

# Example UHV STM Design

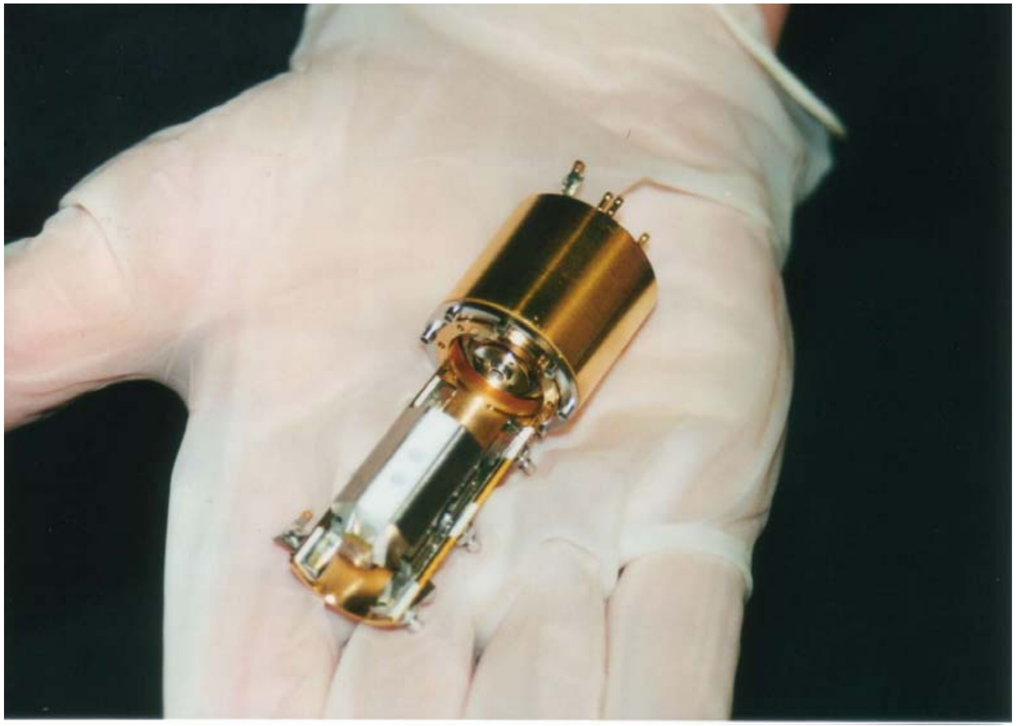

- Homebuilt STM in the Hersam lab at Northwestern University
- STM is a modified Lyding scanner

# Scanner Construction: Piezotubes

Outer tube:
0.650” OD
0.570” ID
0.750” Long

Inner tube:
0.375” OD
0.315” ID
0.750” Long

# Scanner Construction: Base Plug

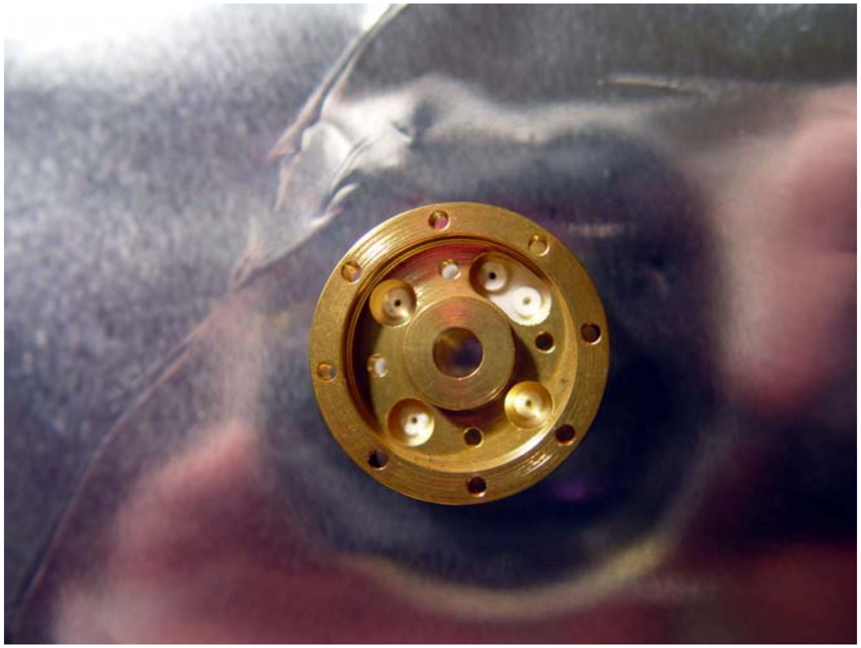

Front View

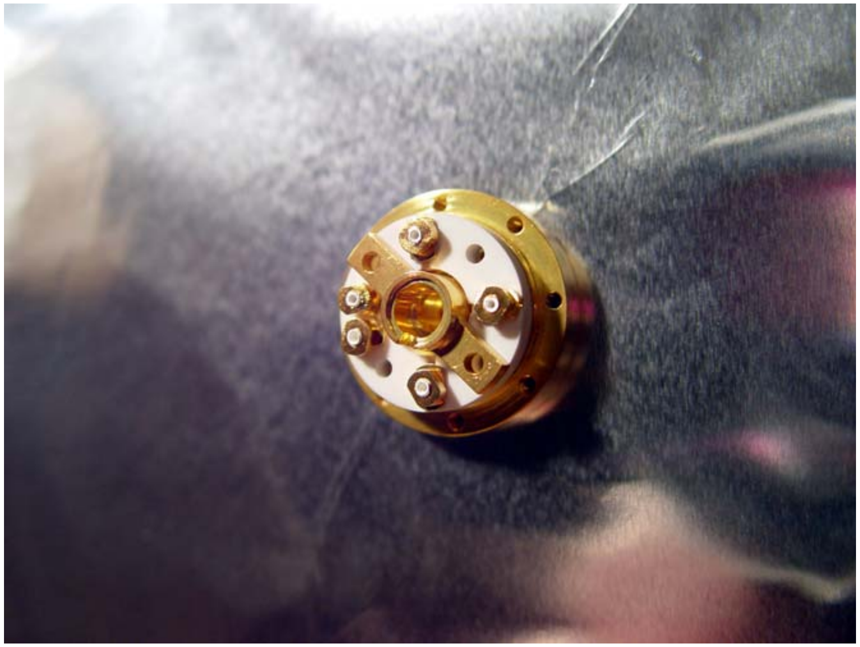

Rear View

# Scanner Construction:
# Piezotubes Soldered into Base Plug

# Scanner Construction:
# Course Translation Platform

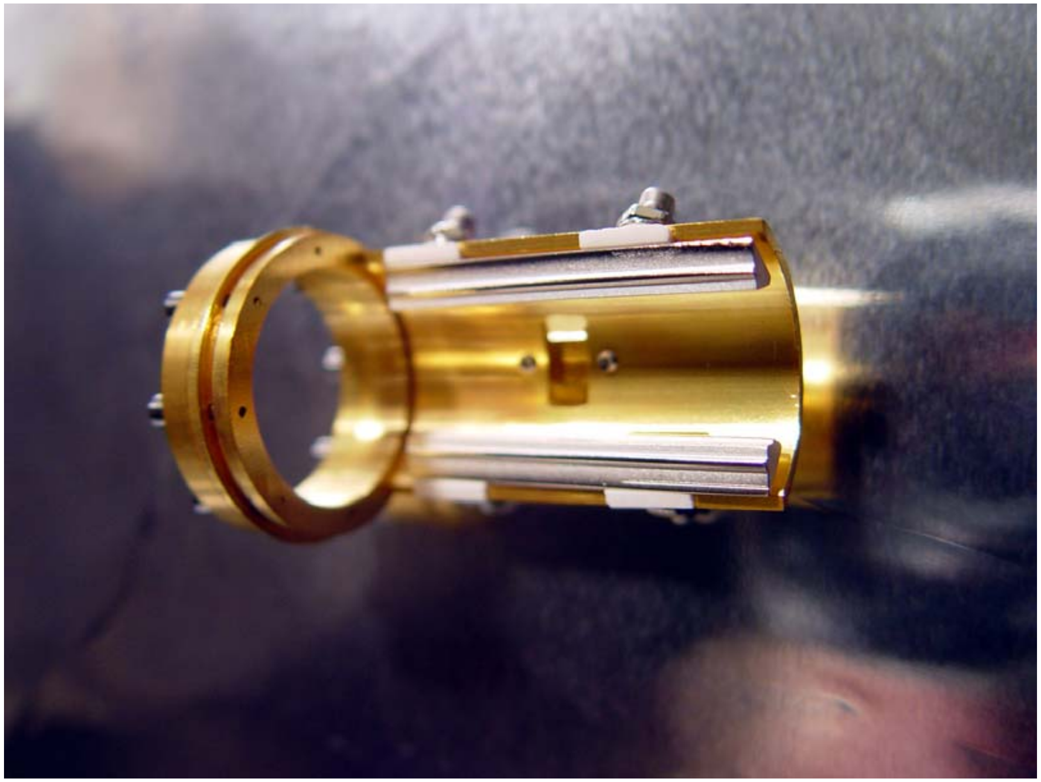

# Scanner Construction: Course Translation Platform Soldered onto Outer Piezotube

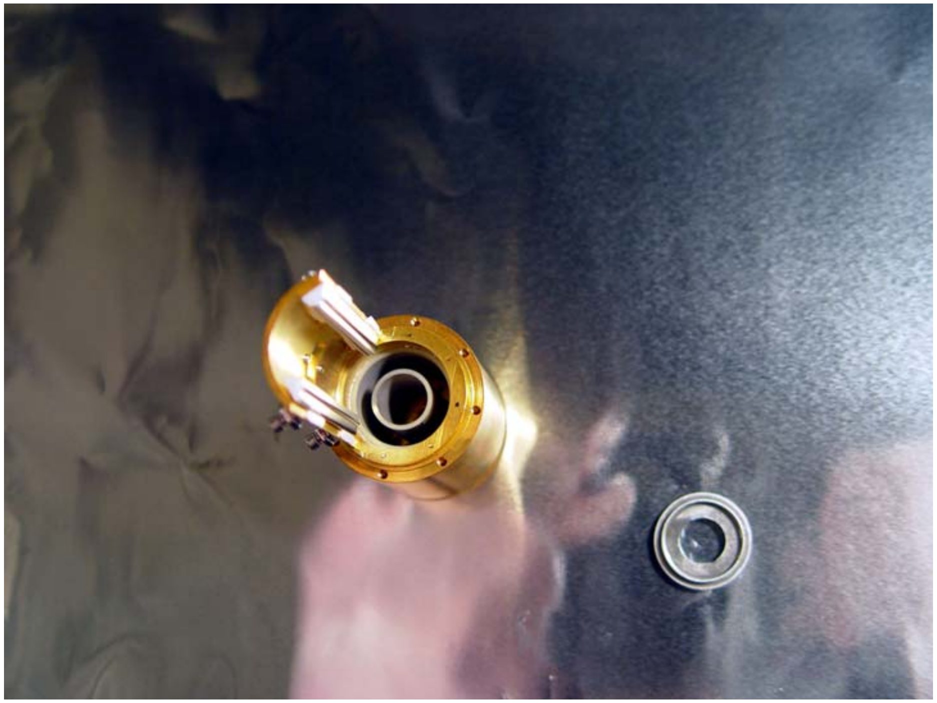

# Scanner Construction:
# End Cap Positioned onto Inner Piezotube

# Scanner Construction:
# Tip Contact Assembly

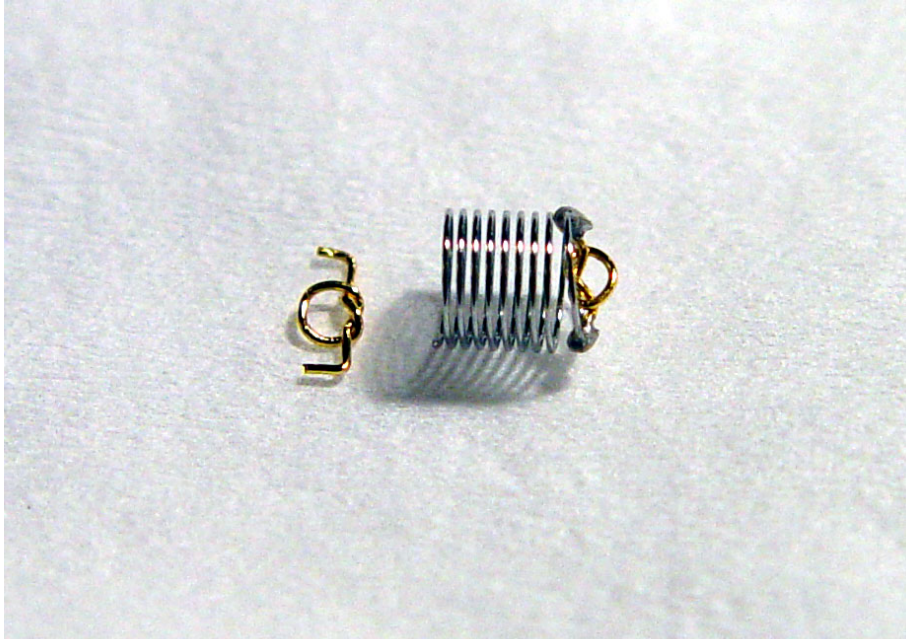

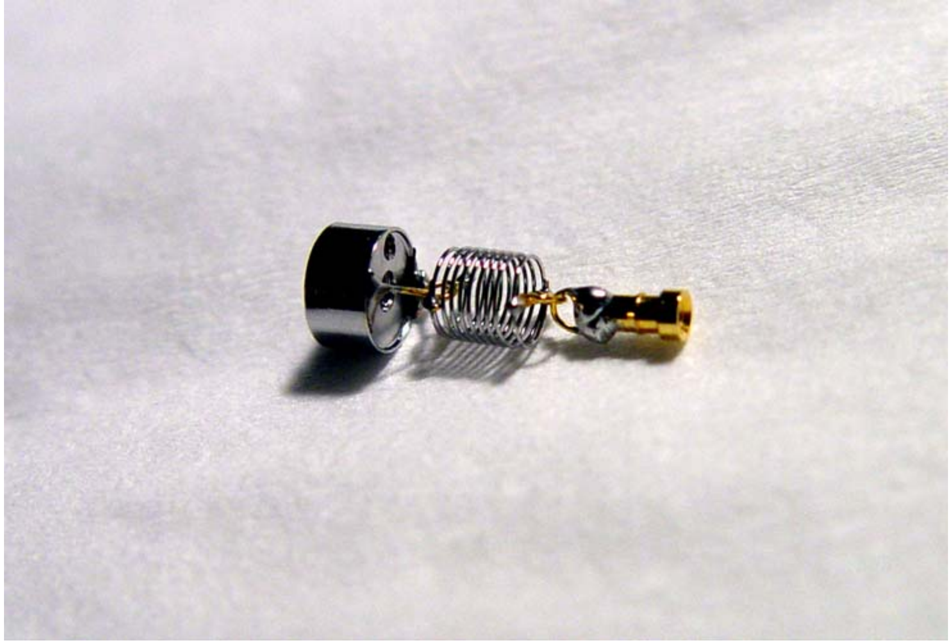

# Scanner Construction:
# Full Tip Assembly

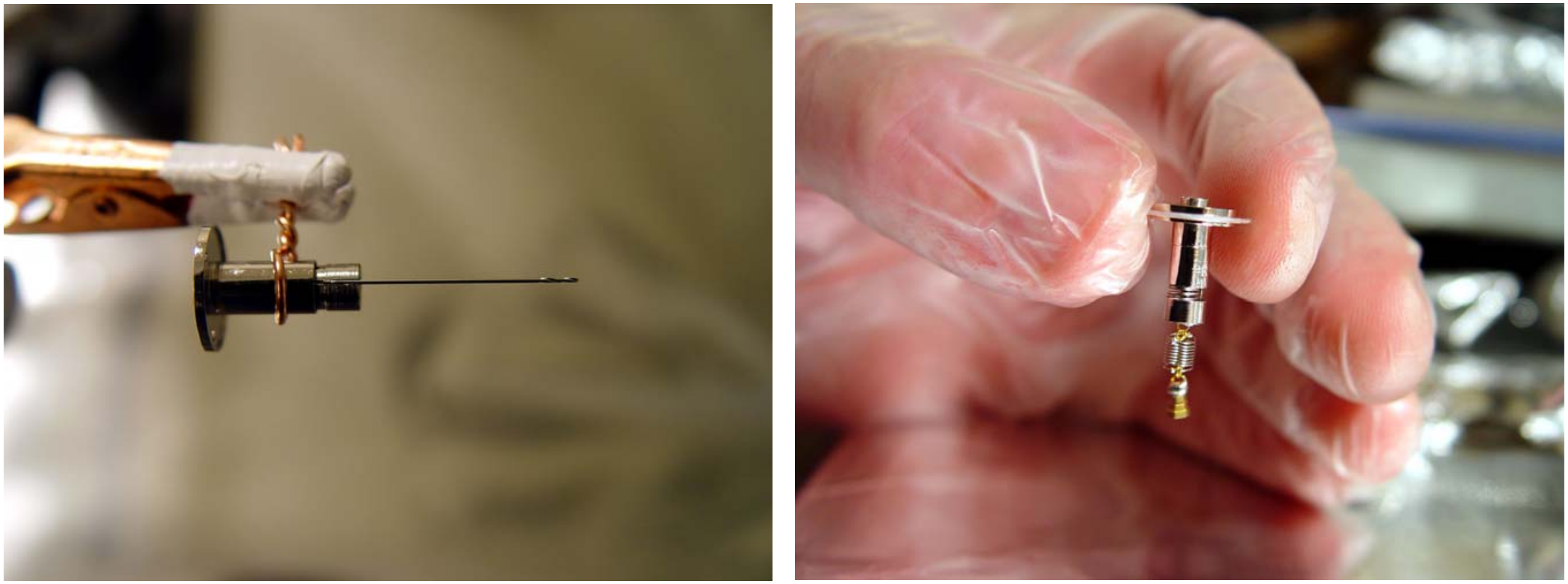

# Scanner Construction: Adjusting Clamping Force on Sapphire Washer and Soldering into Inner Piezotube End Cap

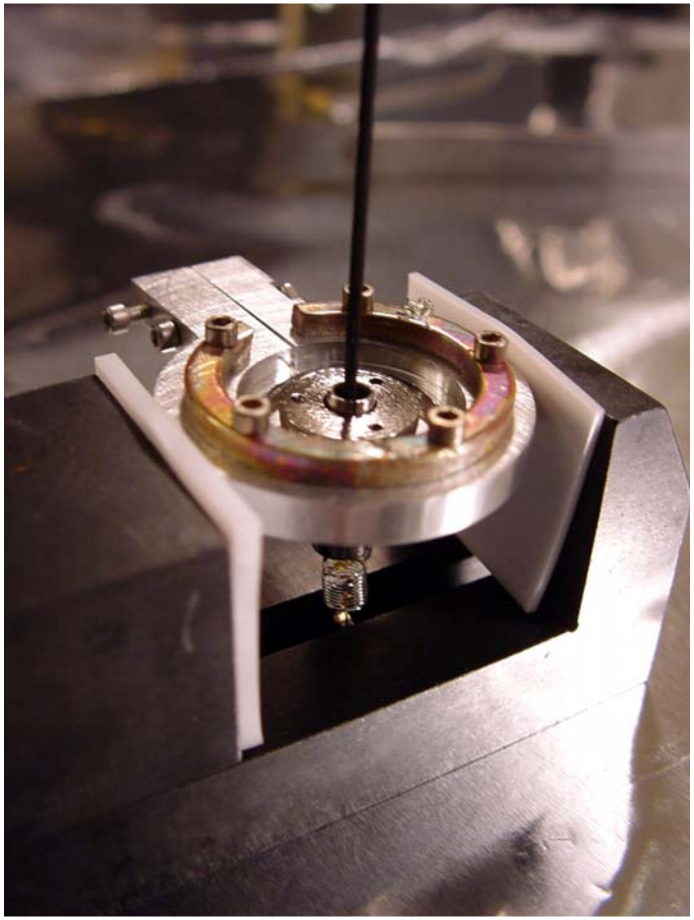

# Scanner Complete

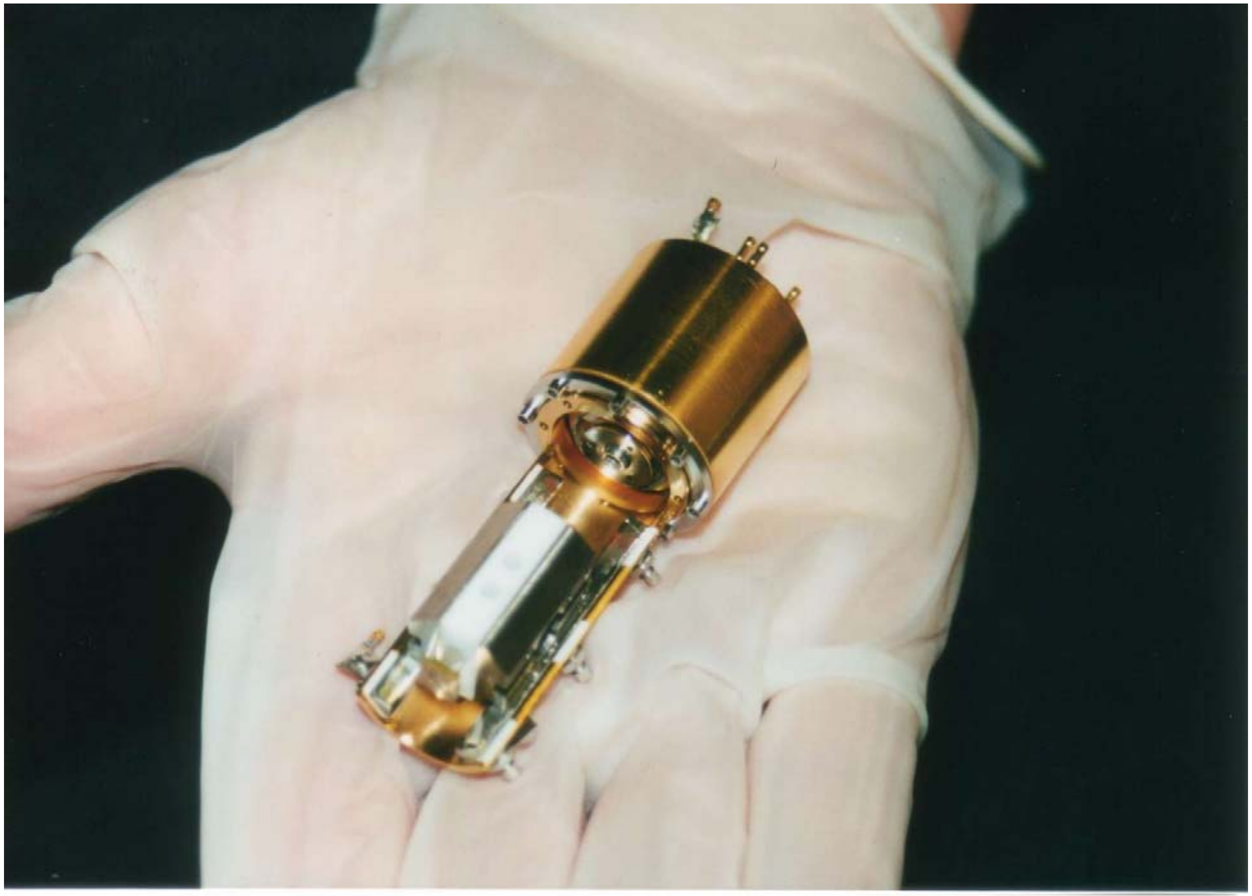

# Cryogenic Variable Temperature UHV STM

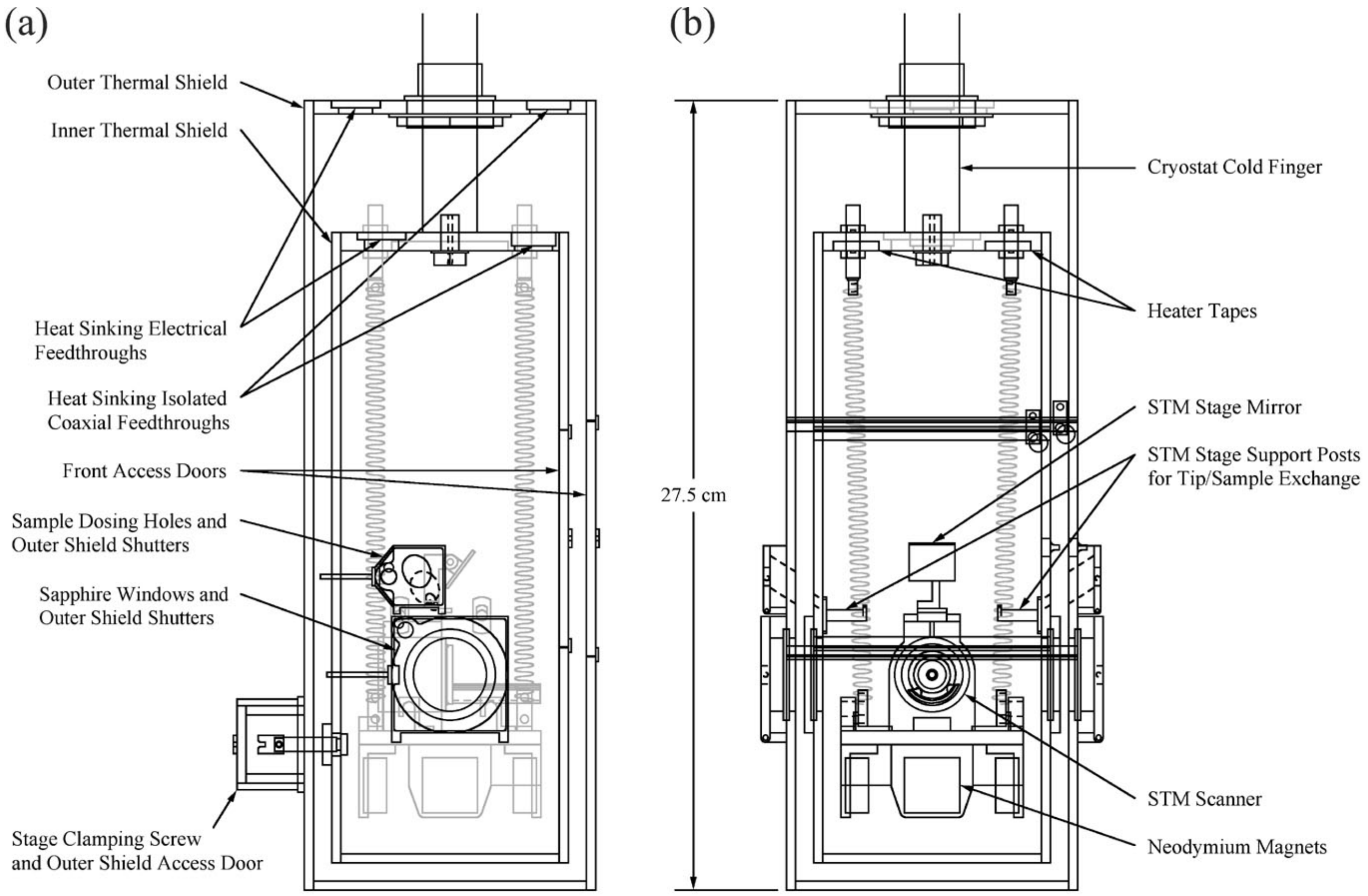

# Vibration Isolation

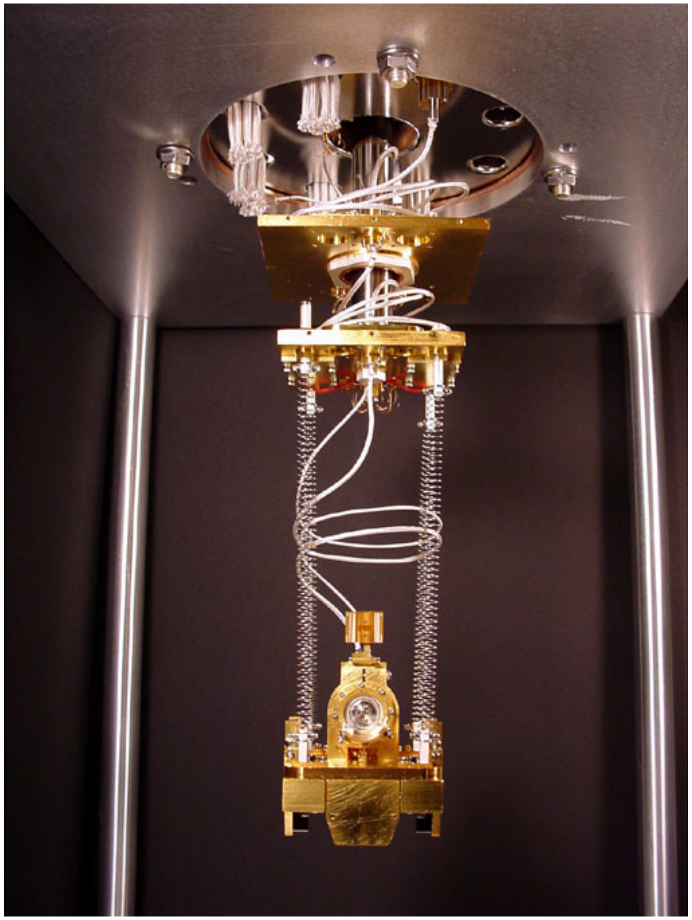

# Detail of Roof Plate

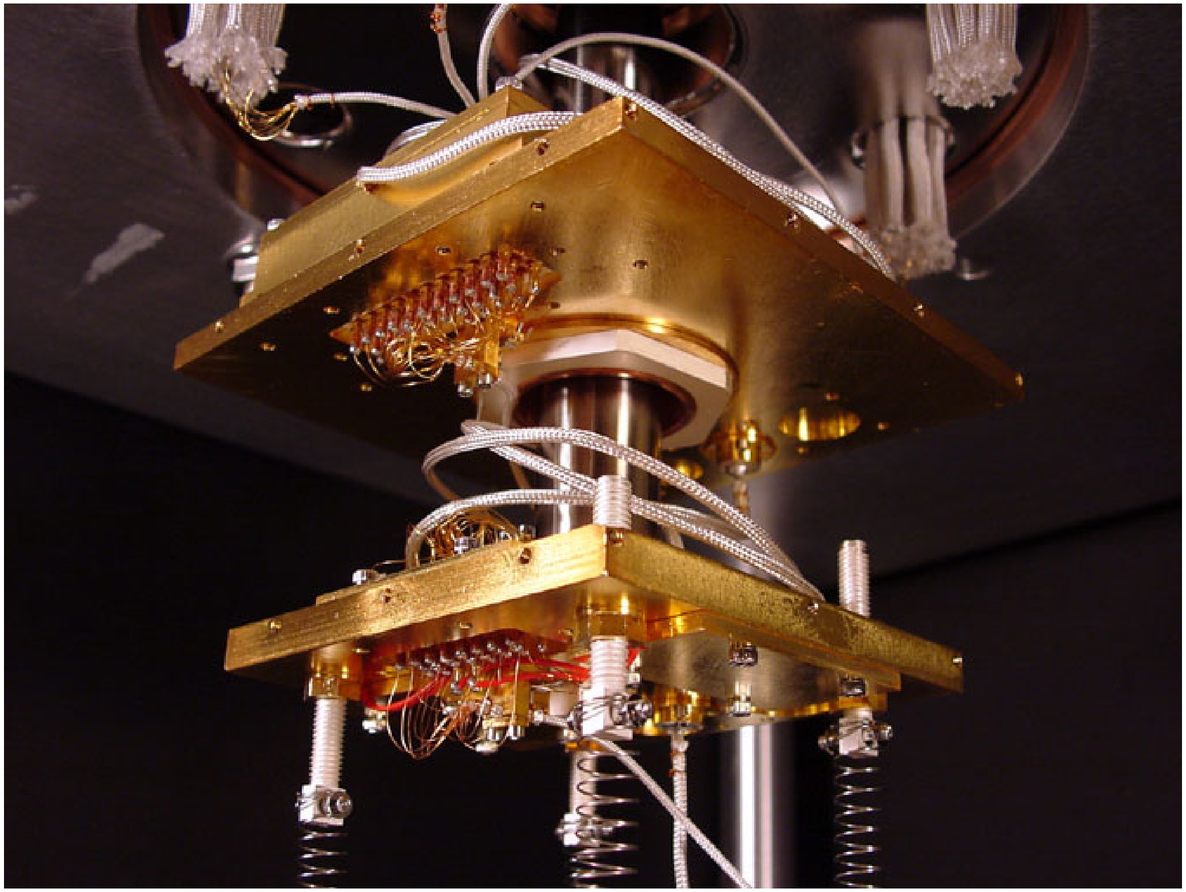

# Detail of STM Stage

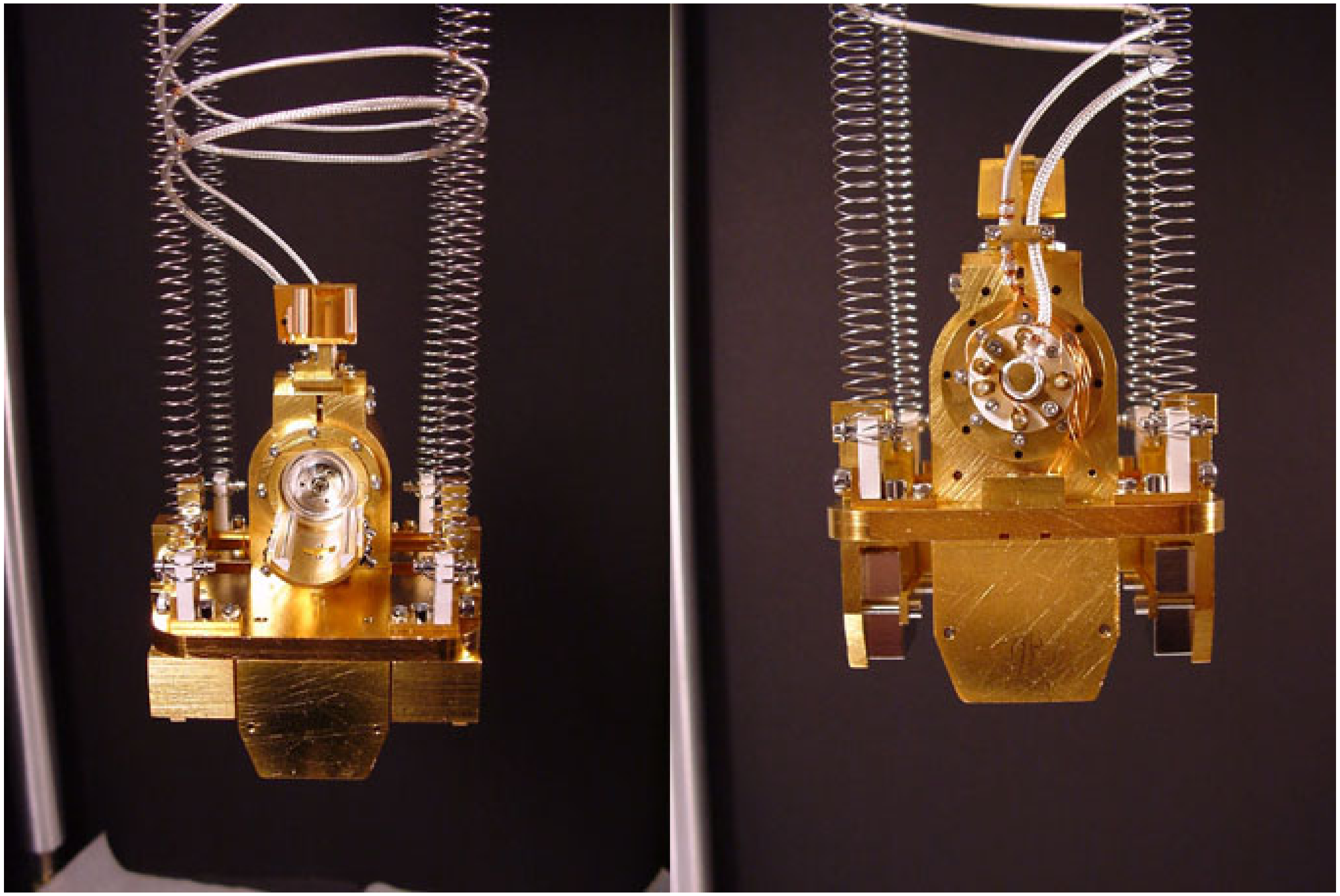

# Thermal Shields with Back Panel Removed

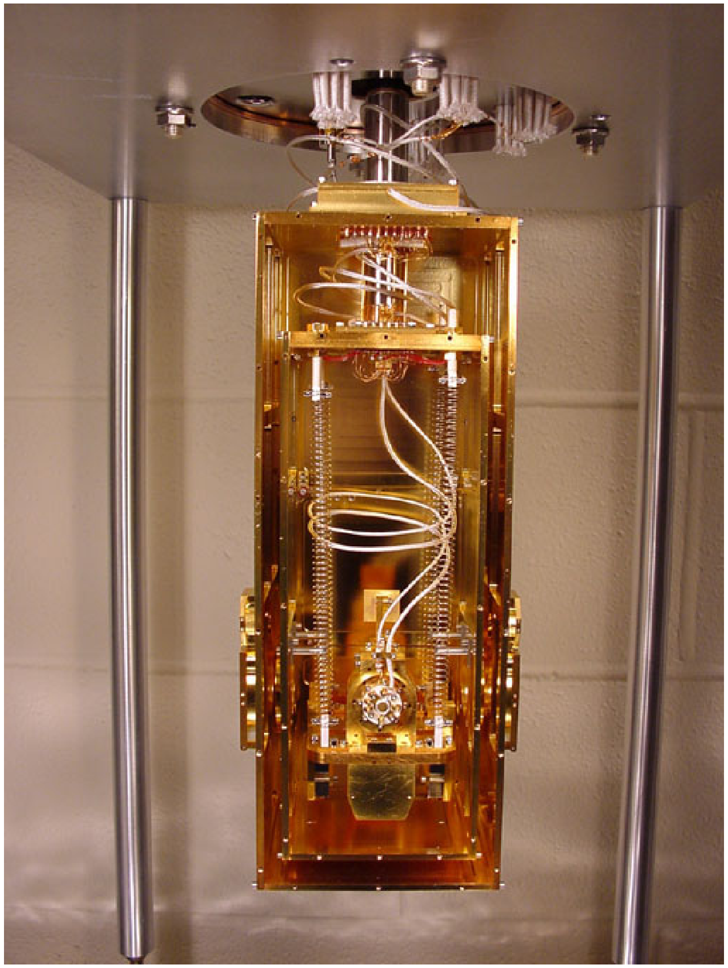

# Stage Locking Screw for Cooldown and Cover

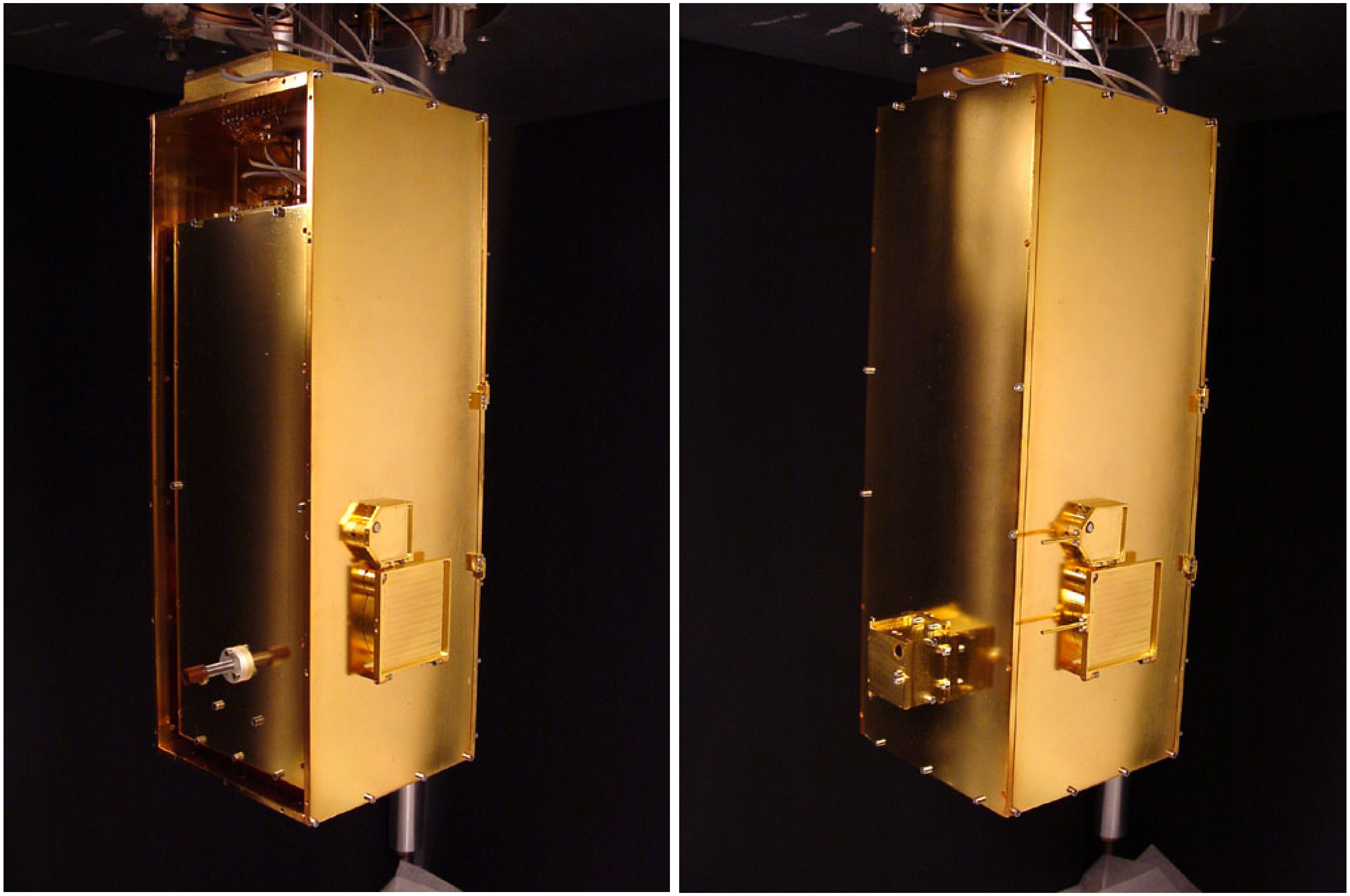

# Rear Door and Shutter Action

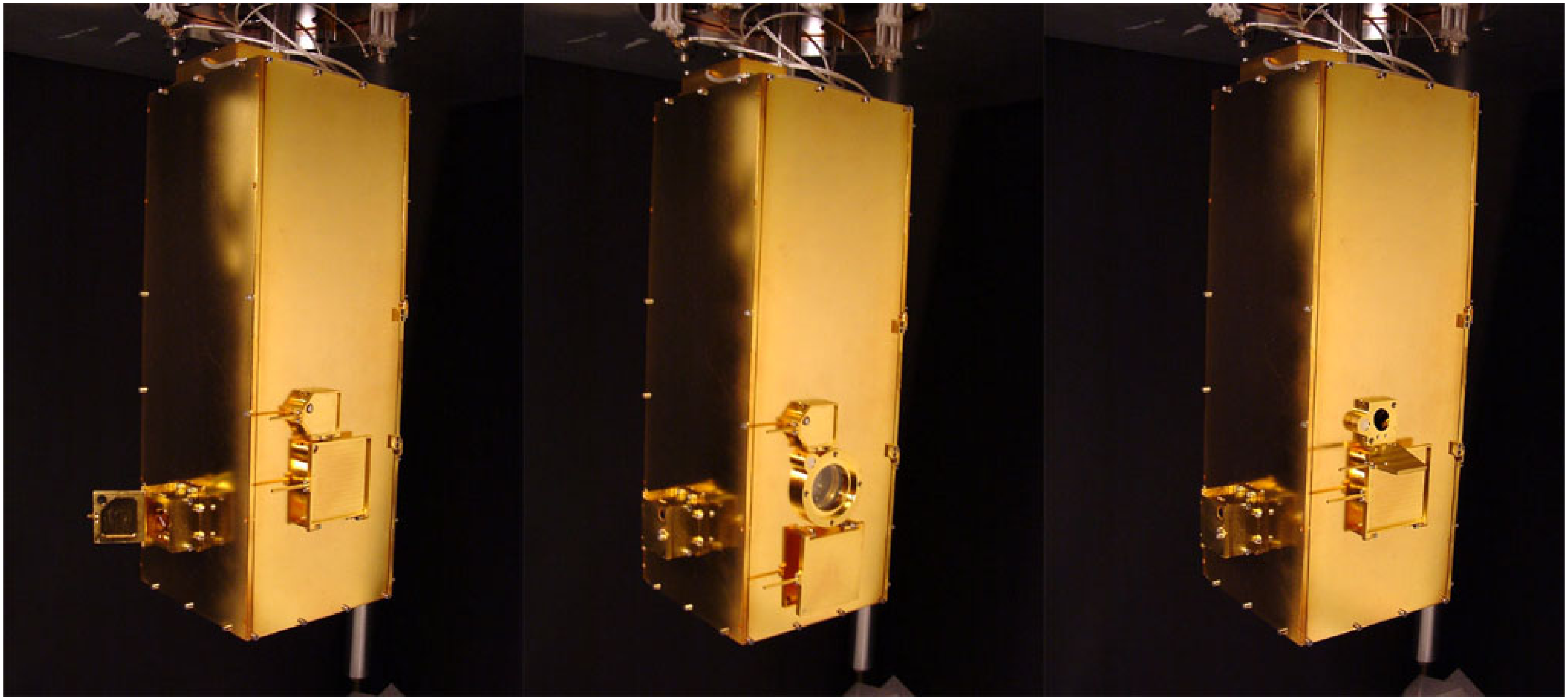

# Front Doors Open for STM Access

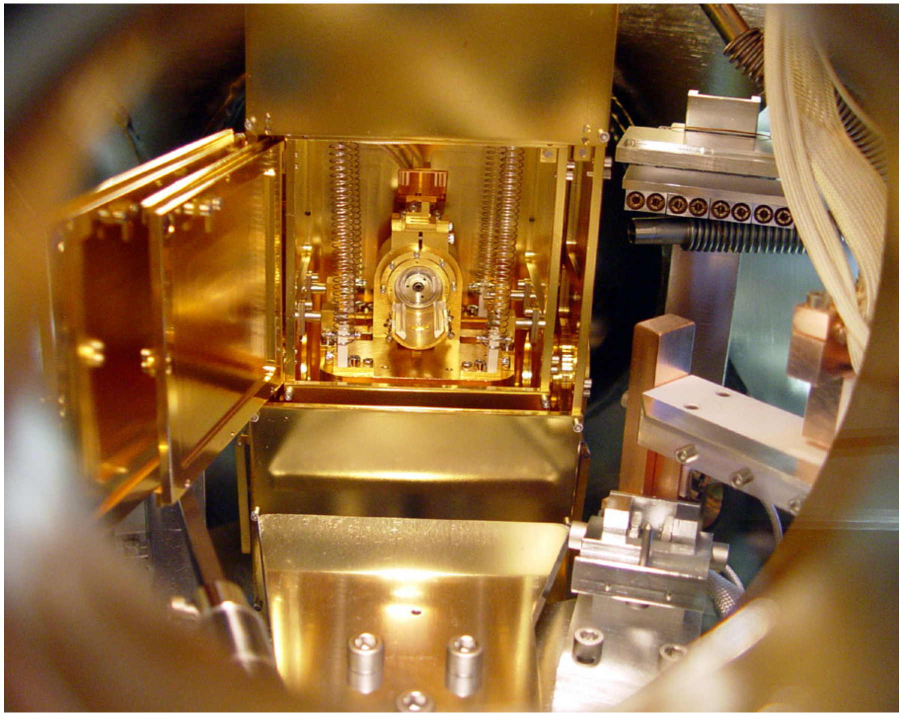

# Sample and Probe Mounted for Scanning

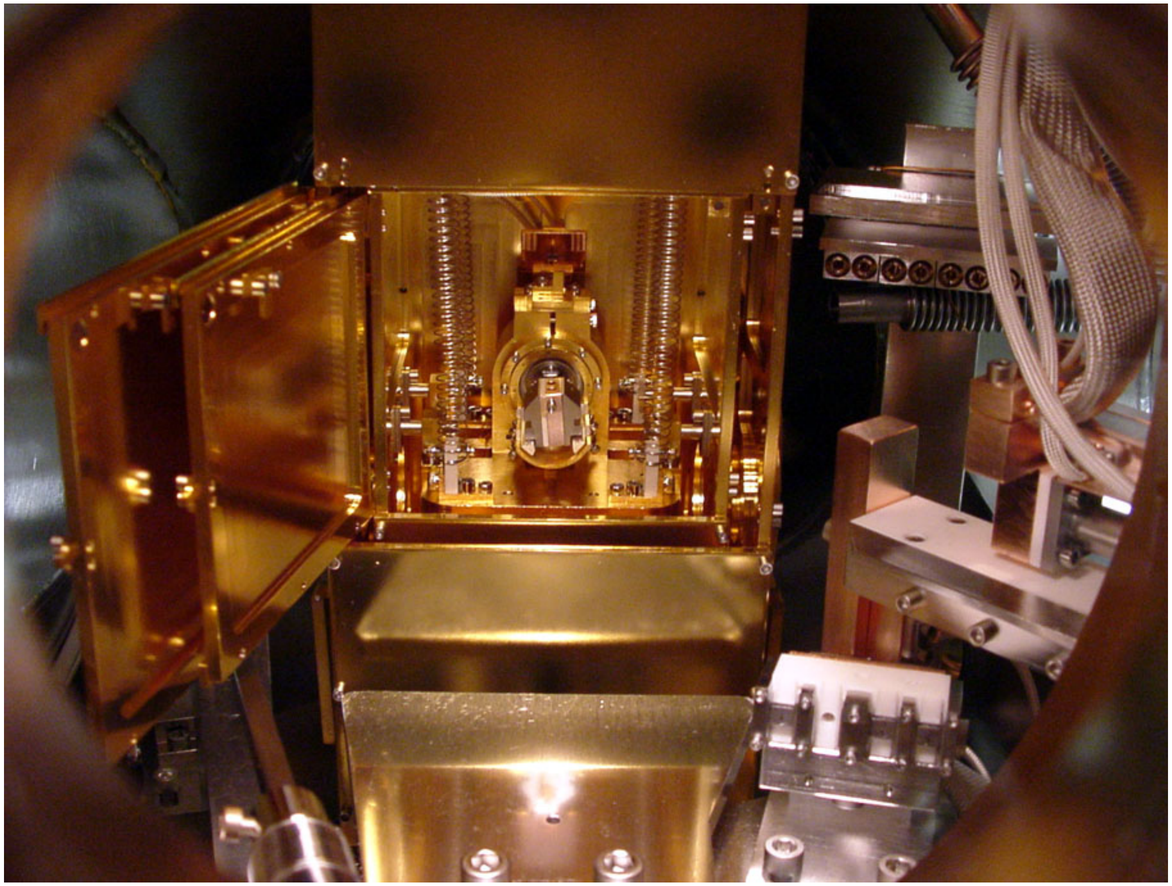

# Mirror Allows for Top-Down View of Tip-Sample Junction

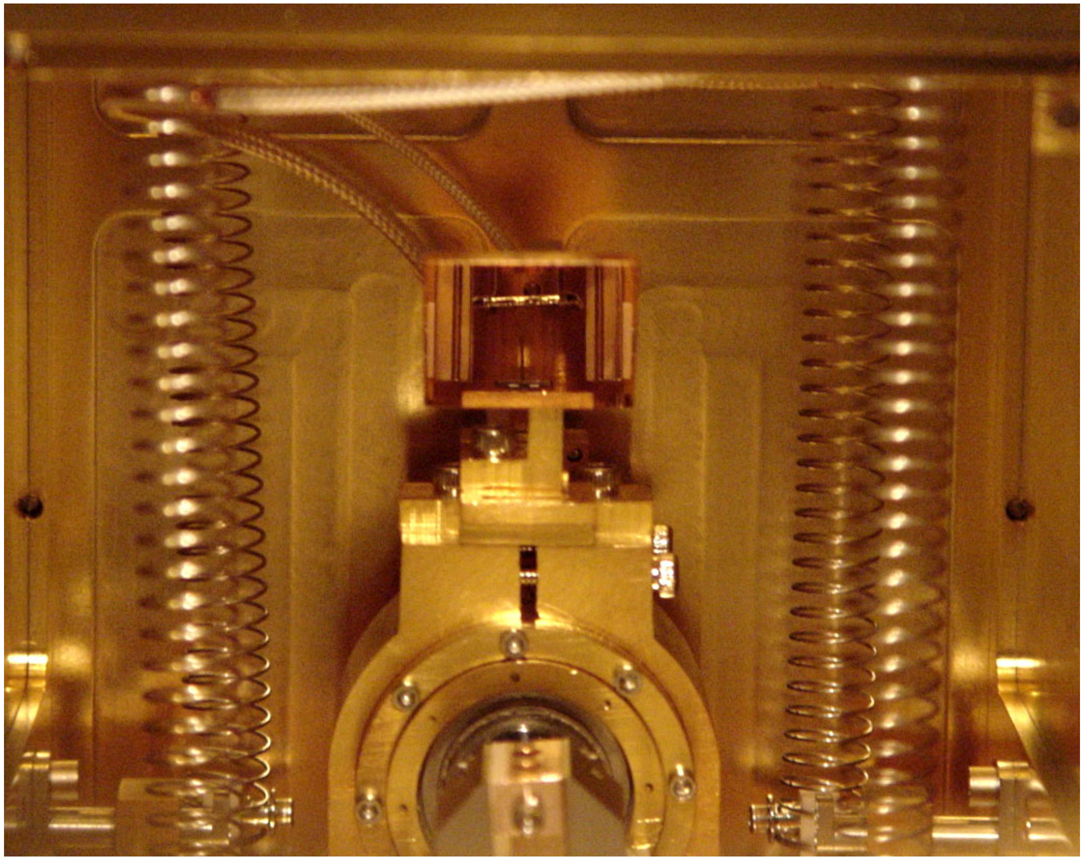

# STM Suspended for Scanning

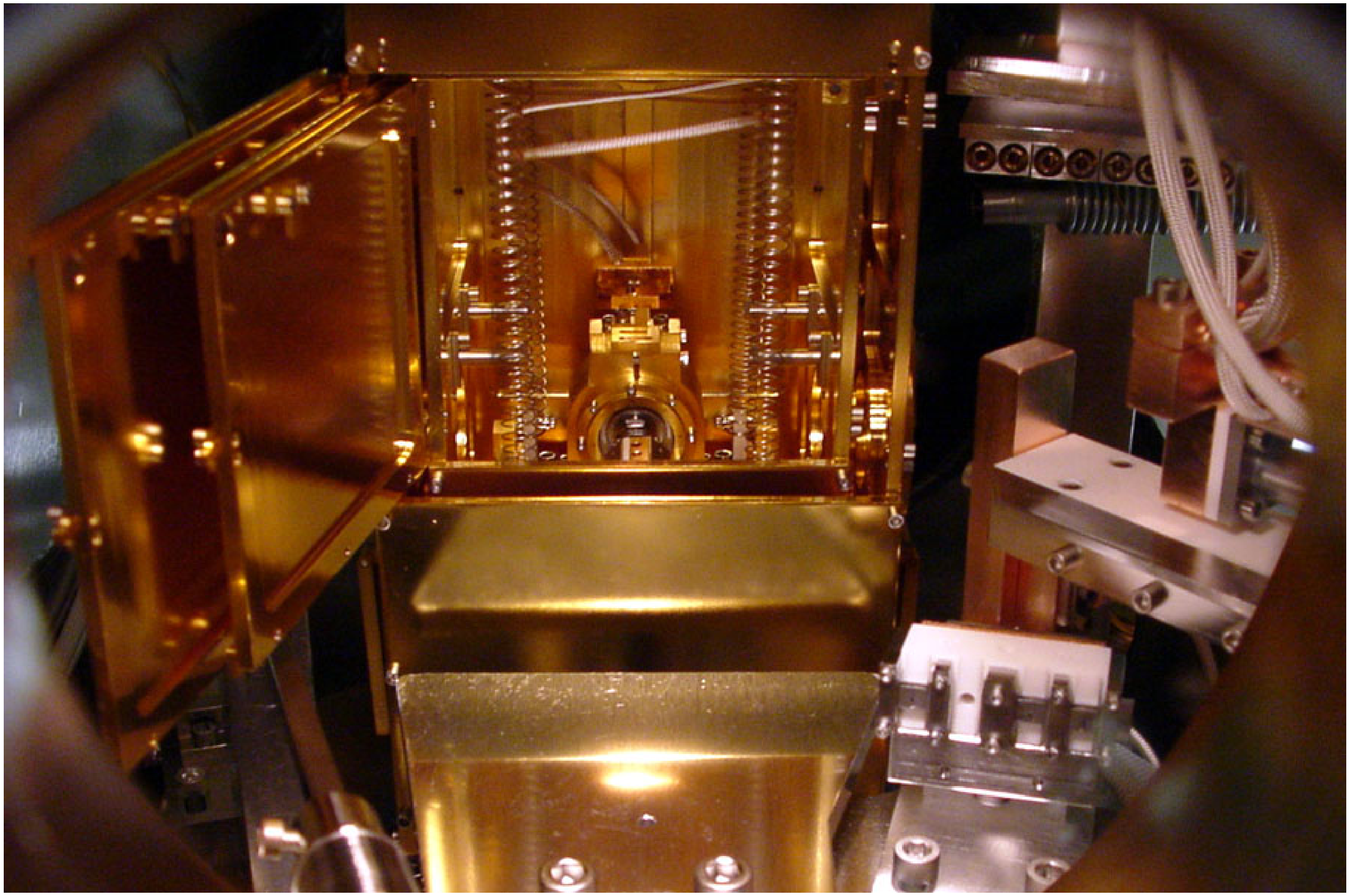

# UHV Chamber and Liquid Helium Dewar

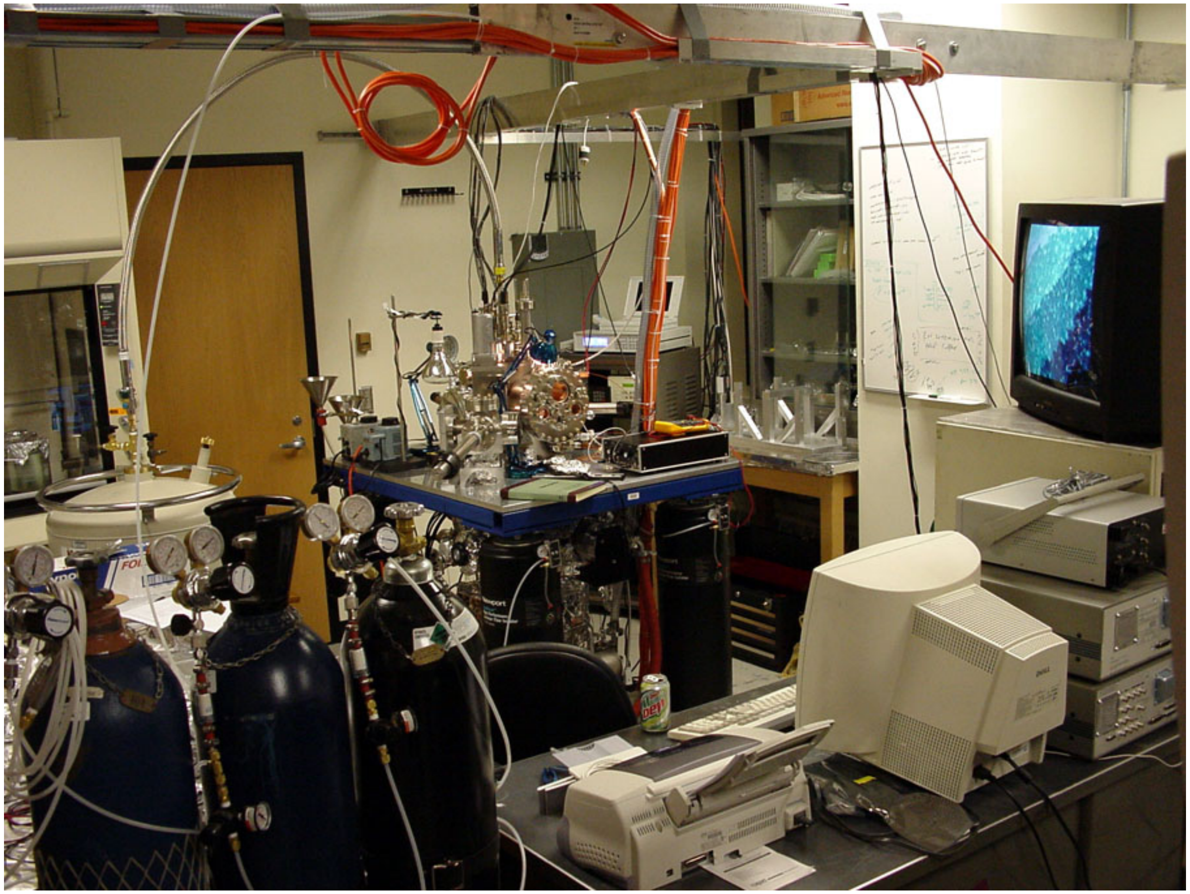

# Scanning Tunneling Microscopy Nanofabrication

Many nanofabrication schemes have been developed with STM (spatial resolution down to the single atom level):

(1) Initially demonstrated by Eigler in 1989
(“IBM” written with atoms at cryogenic temperatures)

(2) Room temperature atom removal from Si(111) by Avouris

(3) Field evaporation of gold

(4) Electron stimulated desorption of hydrogen from Si(100)

# Tunable Bond Formation with STM

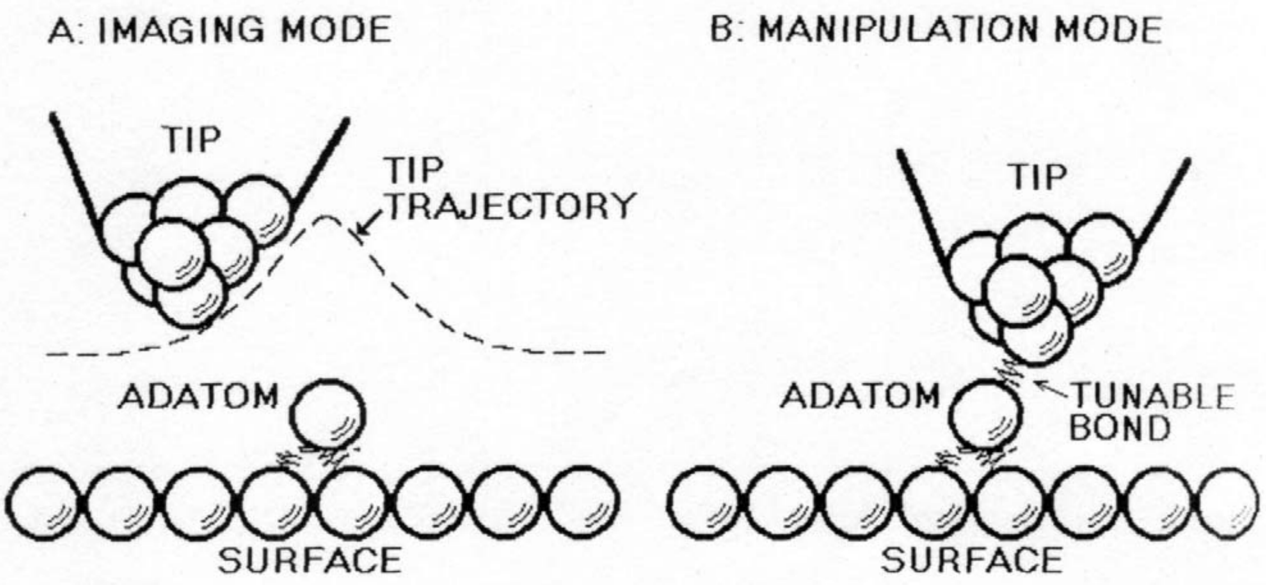

**FIGURE 2.** (A) In the imaging mode the tip is stabilized far enough above the surface so that the interaction between the tip and the adatom is negligible. (B) In the manipulation mode the tip is brought close enough to the adatom to drag the adatom along the surface. The force exerted on the adatom by the tip is due to the partially formed chemical bond between the tip and the adatom.

G. Timp, *Nanotechnology*, Chapter 11

# Sliding Adatoms with STM

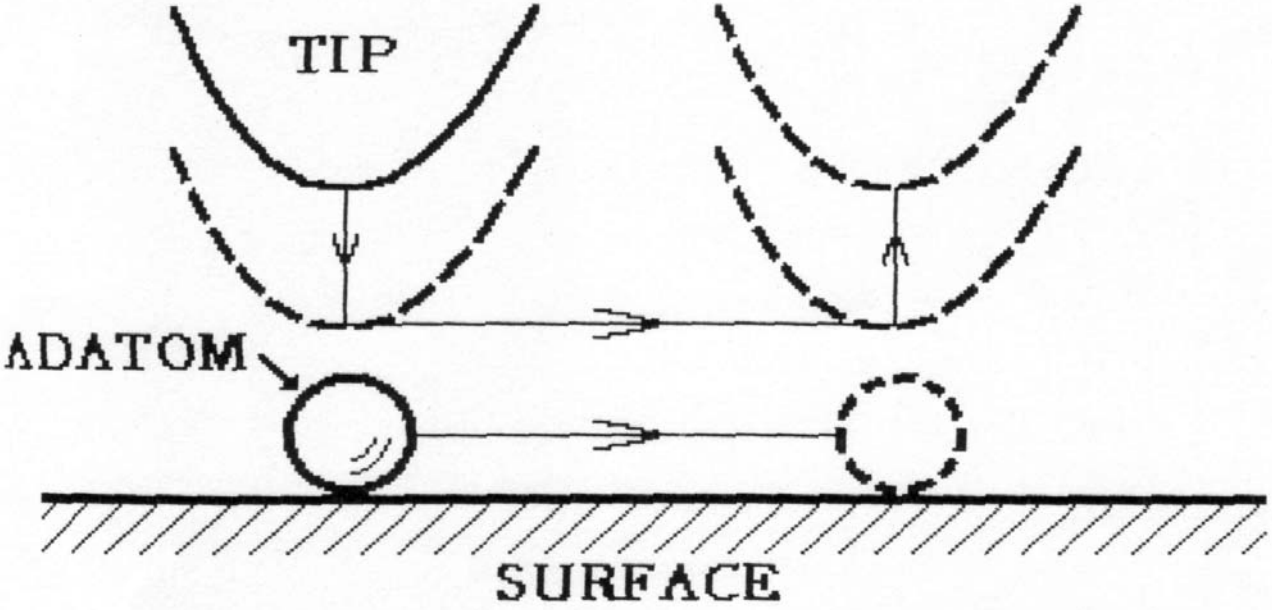

**FIGURE 3.** Schematic of the sliding process. The tip is placed above the adatom and then lowered to an empirically determined height at which the attractive interaction between the tip and the adatom is sufficient to pull the adatom along the surface. Once the adatom is moved to its final location, the tip is raised back to the height used for imaging, effectively terminating the tip-adatom interaction.

G. Timp, *Nanotechnology*, Chapter 11

# The First Atom Moved with STM

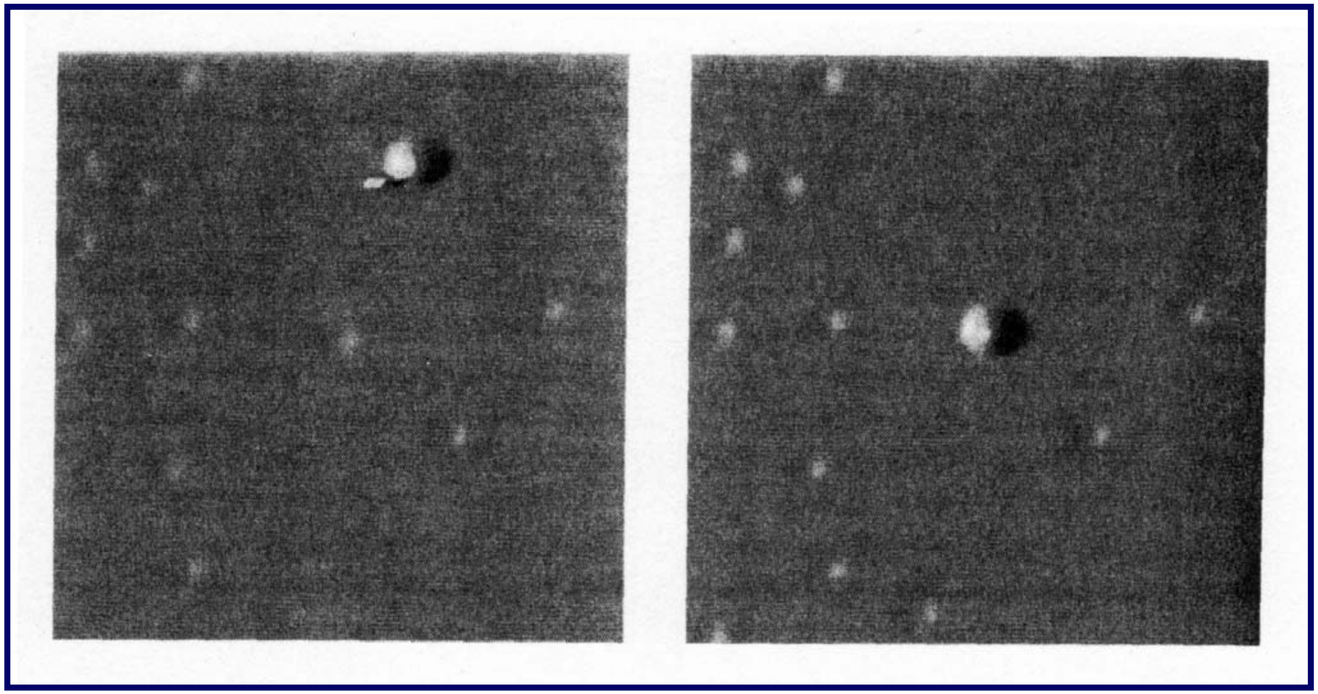

Xenon on platinum → requires a defect to prevent tip-induced motion under normal scanning conditions

G. Timp, *Nanotechnology*, Chapter 11

# STM Manipulation of Xenon on Nickel

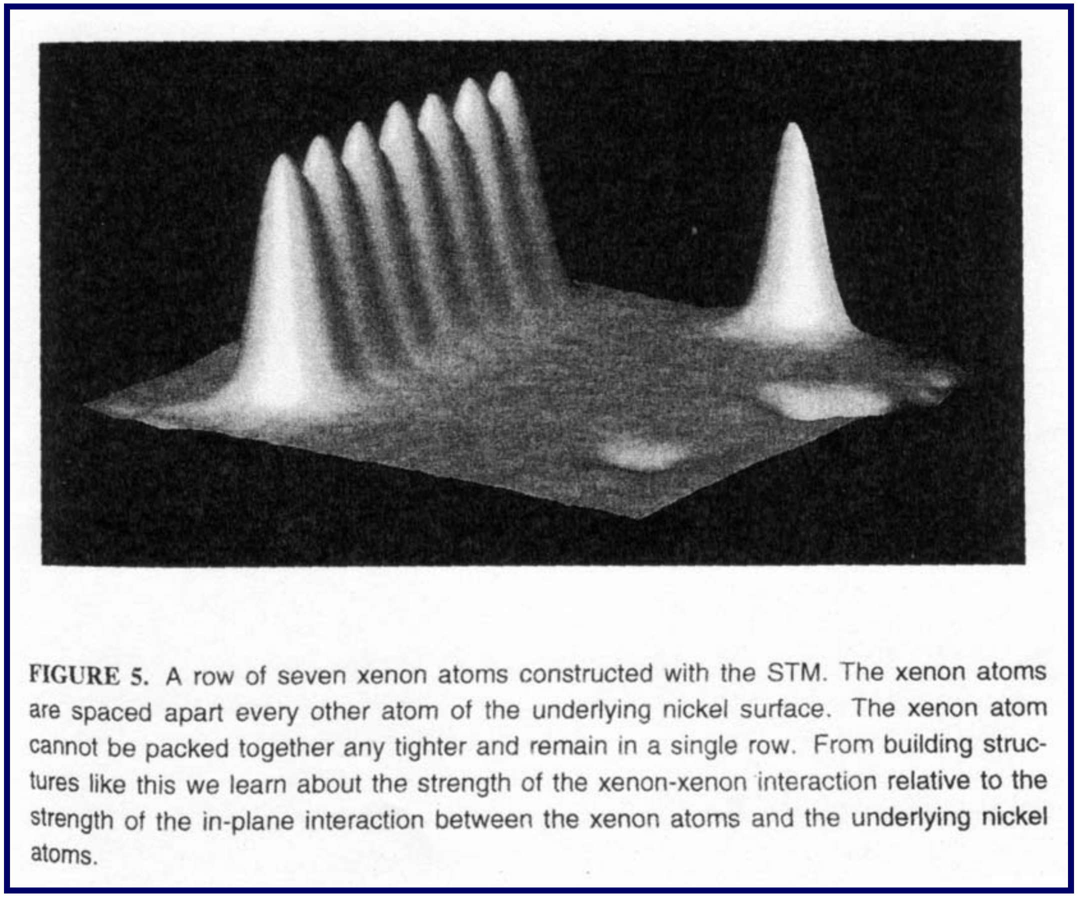

**FIGURE 5.** A row of seven xenon atoms constructed with the STM. The xenon atoms are spaced apart every other atom of the underlying nickel surface. The xenon atom cannot be packed together any tighter and remain in a single row. From building structures like this we learn about the strength of the xenon-xenon interaction relative to the strength of the in-plane interaction between the xenon atoms and the underlying nickel atoms.

G. Timp, *Nanotechnology*, Chapter 11

# Nanograffiti

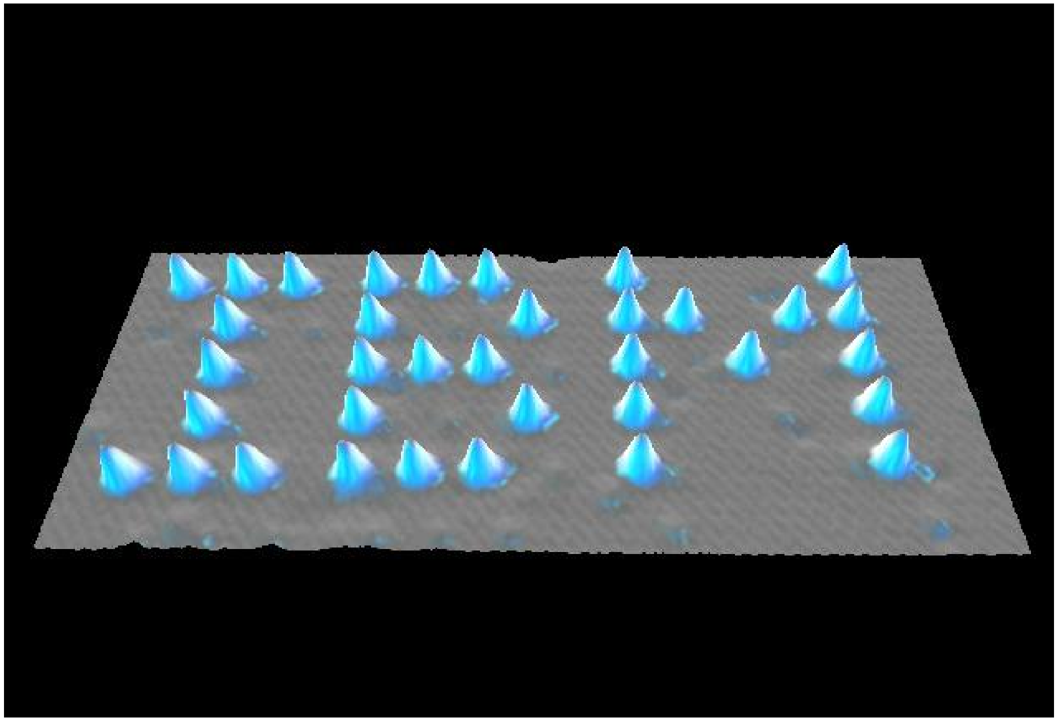

Xenon atoms on Nickel (110)

*Kanji for atom:*

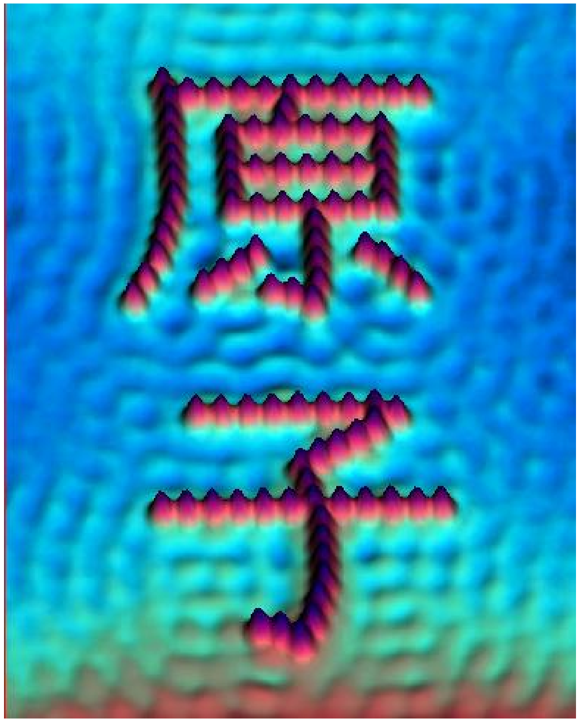

Fe atoms on Cu(111)

Don Eigler, IBM Alamden, http://www.almaden.ibm.com/vis/stm/atomo.html

# Quantum Corrals

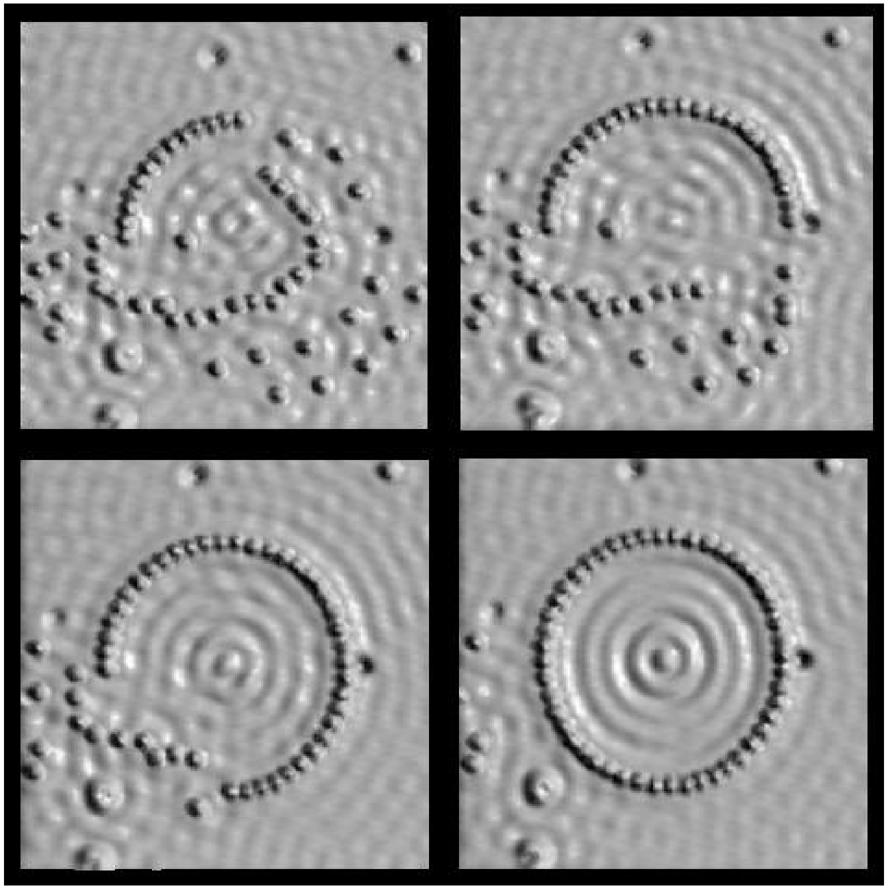

**Fe atoms on Cu(111)**

Don Eigler, IBM Alamden, http://www.almaden.ibm.com/vis/stm/atomo.html

# Quantum Mirage (Kondo Resonance)

*Topography:*

*dI/dV:*

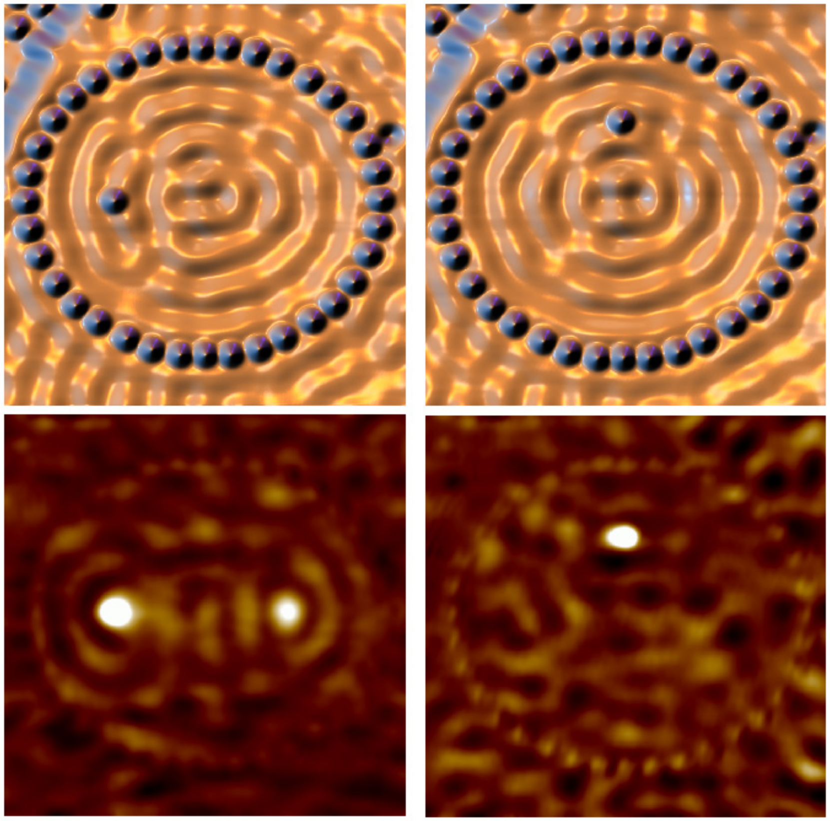

**Co atoms on Cu(111)**

Don Eigler, IBM Alamden, http://www.almaden.ibm.com/vis/stm/atomo.html

# Room Temperature Manipulation of Si(111)

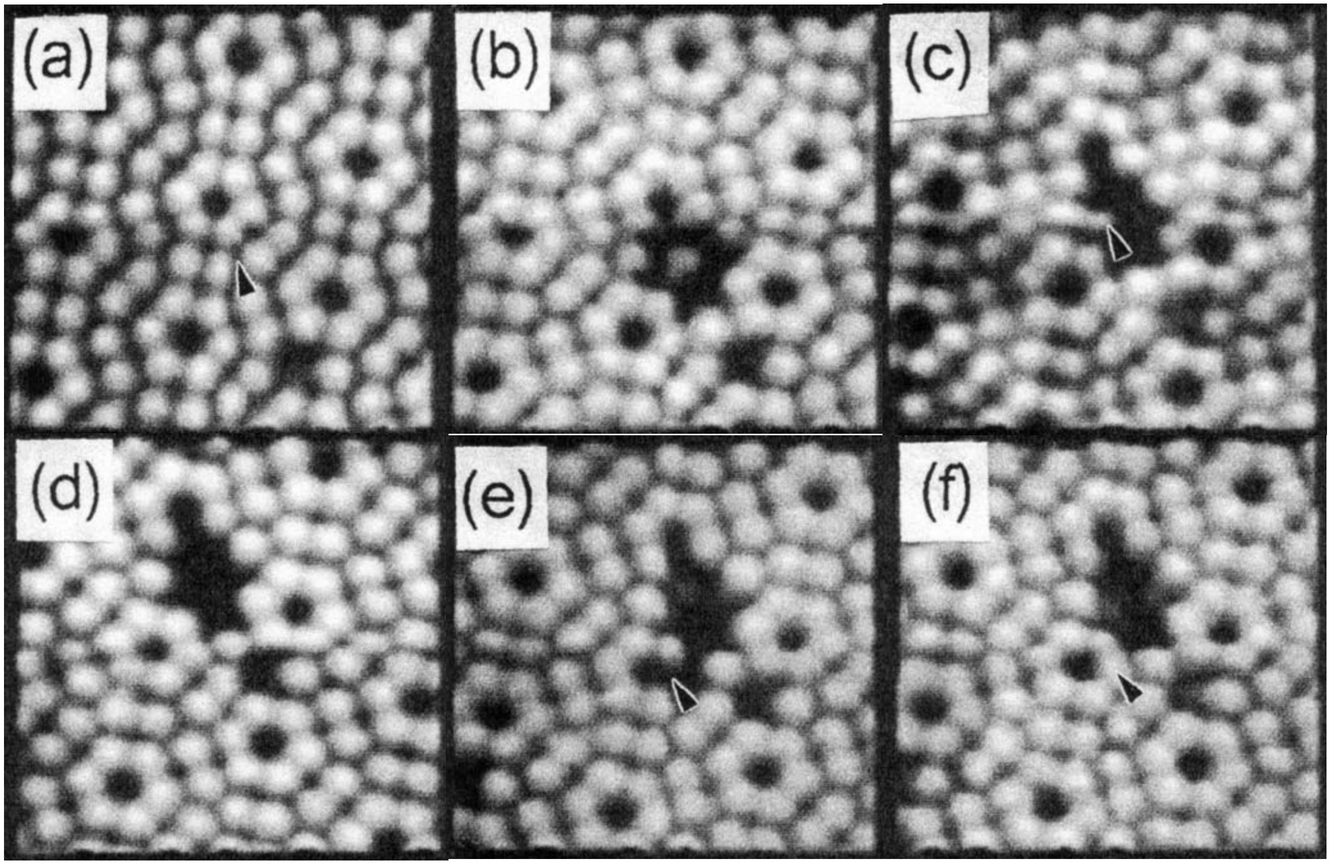

C. Julian Chen, *Introduction to Scanning Tunneling Microscopy*

# Field Evaporation of Gold

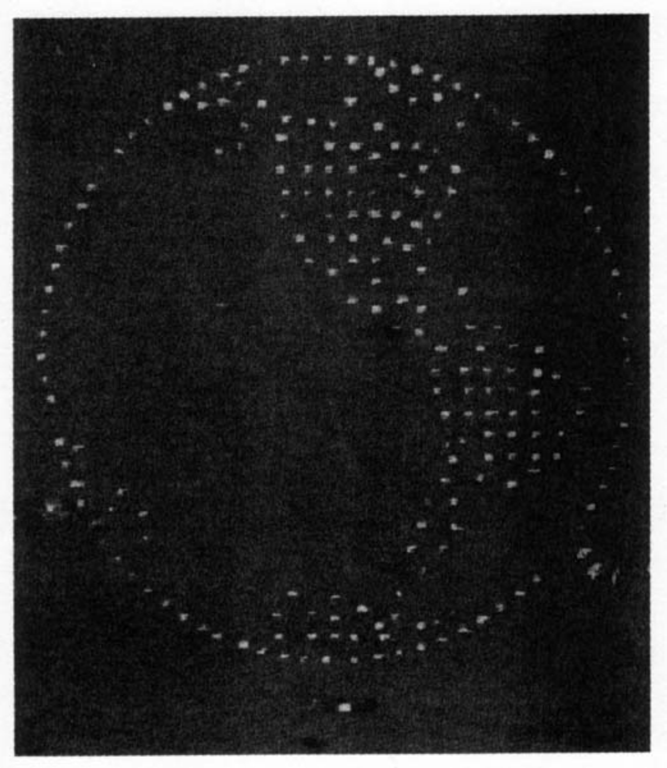

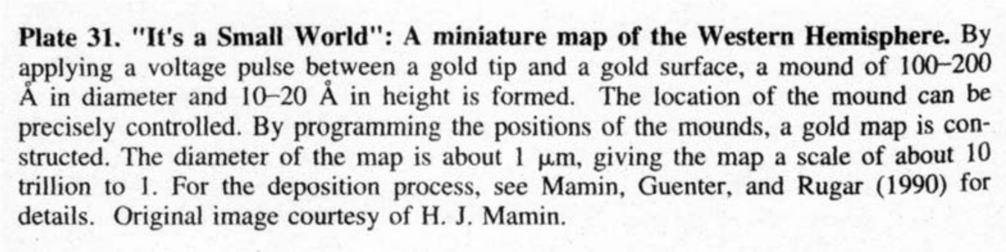

**Plate 31. "It's a Small World": A miniature map of the Western Hemisphere.** By applying a voltage pulse between a gold tip and a gold surface, a mound of 100–200 Å in diameter and 10–20 Å in height is formed. The location of the mound can be precisely controlled. By programming the positions of the mounds, a gold map is constructed. The diameter of the map is about 1 μm, giving the map a scale of about 10 trillion to 1. For the deposition process, see Mamin, Guenter, and Rugar (1990) for details. Original image courtesy of H. J. Mamin.

C. Julian Chen, *Introduction to Scanning Tunneling Microscopy*

# Hydrogen Passivated Si(100)

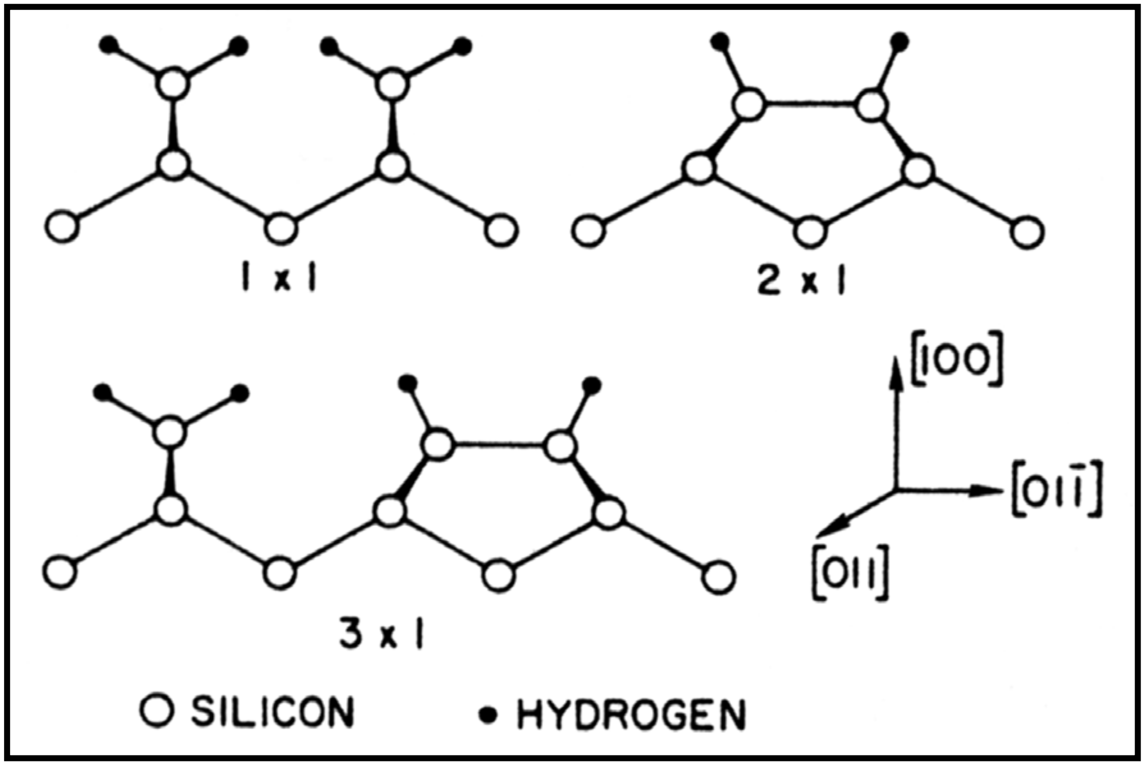

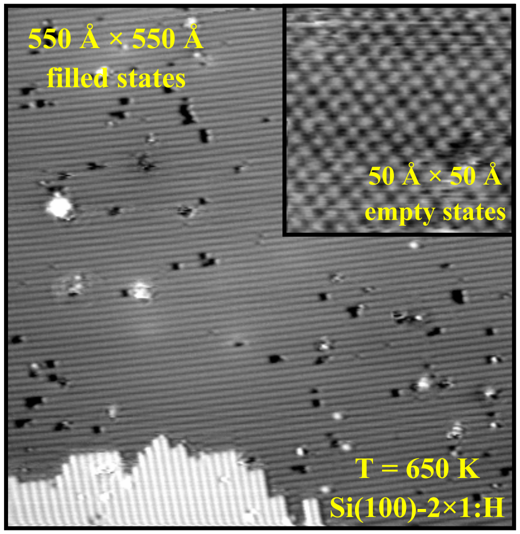

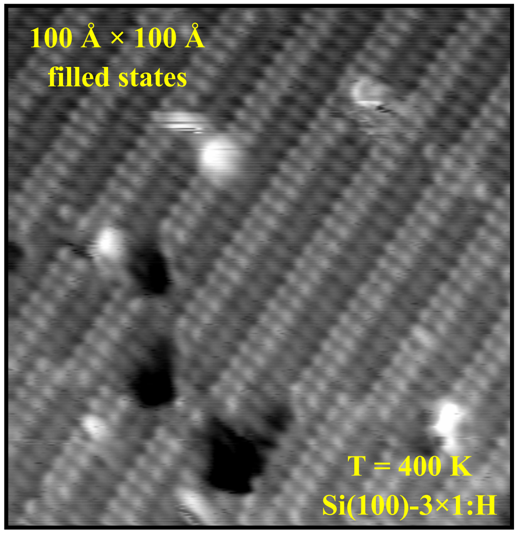

# STM Nanolithography on Si(100)-2×1:H

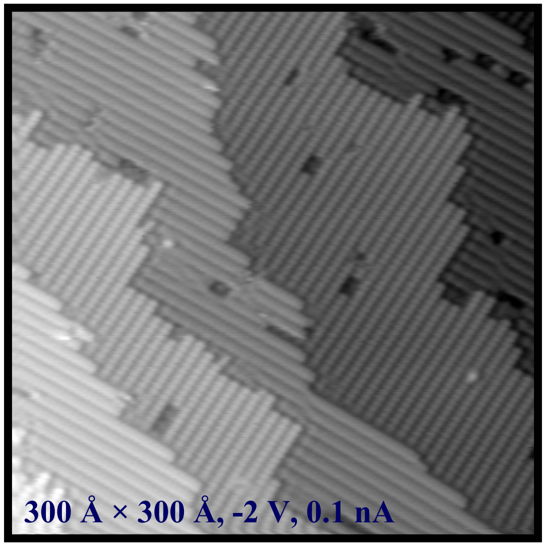

A relatively stable and unreactive surface is produced by hydrogen passivating the Si(100)-2×1 surface in ultra-high vacuum (UHV).

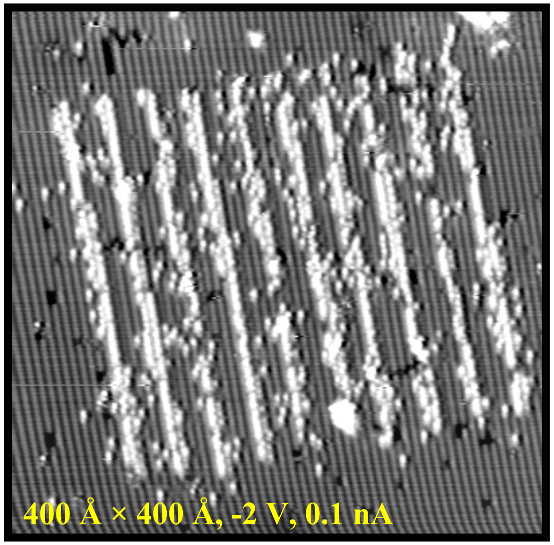

Highly reactive "dangling bonds" are created by using the STM as a highly localized electron beam.

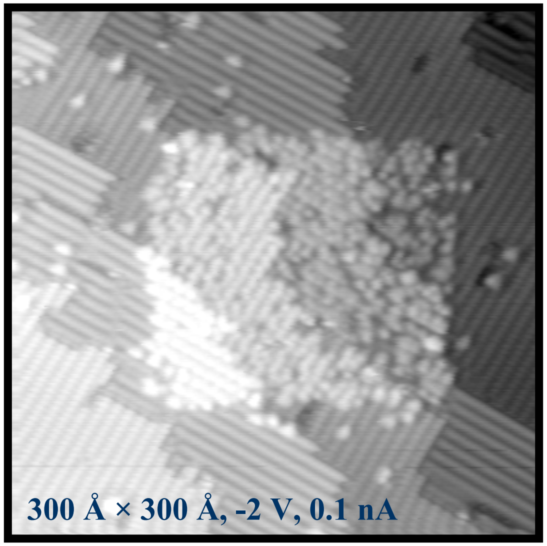

The linewidth and desorption yield are a function of the incident electron energy, the current density, and the total electron dose.

- **Selective chemistry can be accomplished on patterned areas.**

J. W. Lyding, *et al.*, *Appl. Phys. Lett.*, **64**, 2010 (1994).

# Hydrogen Desorption Mechanisms

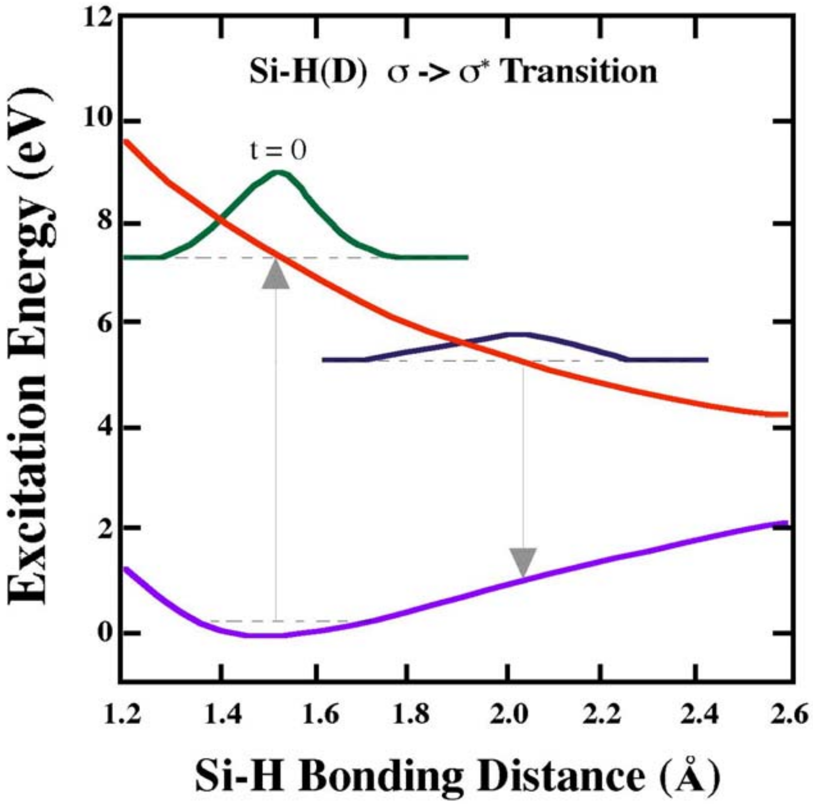

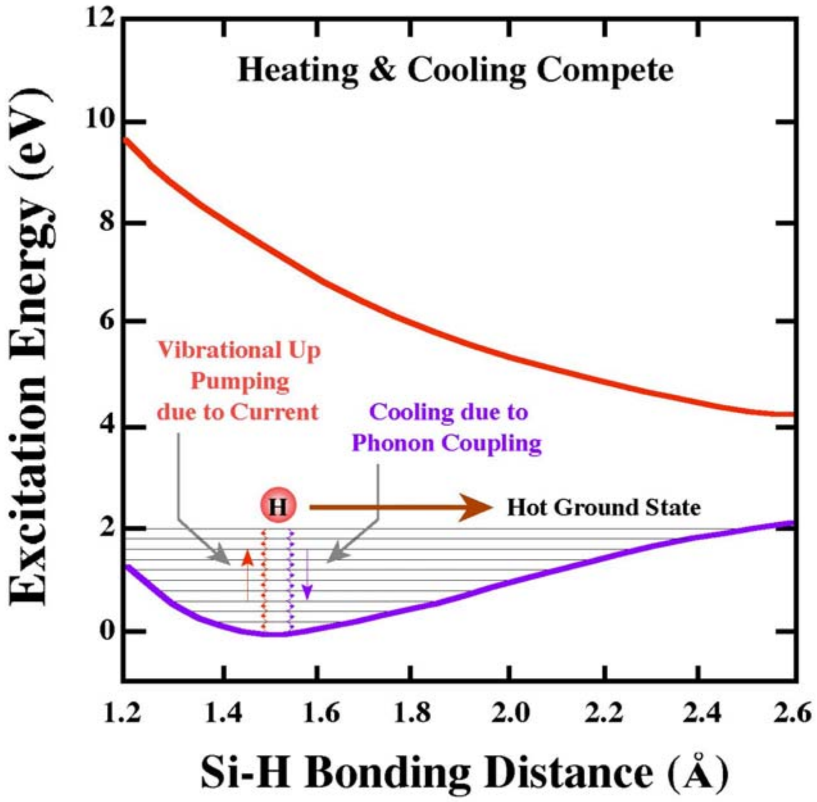

# Selective Molecular Adsorption of Norbornadiene on Silicon

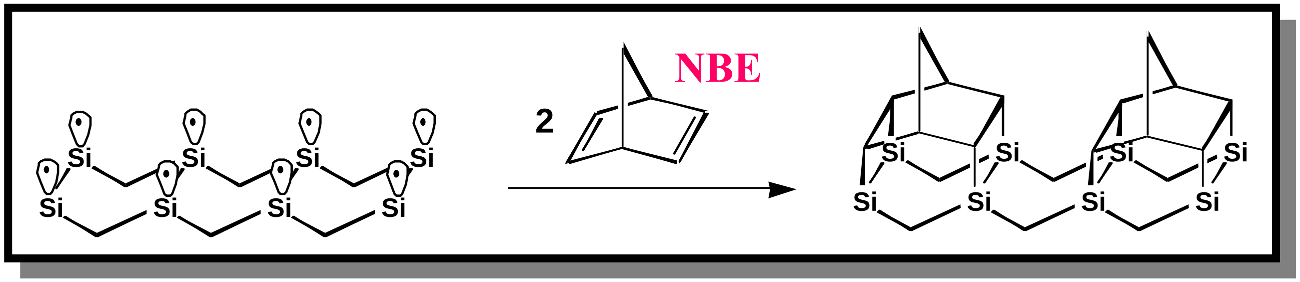

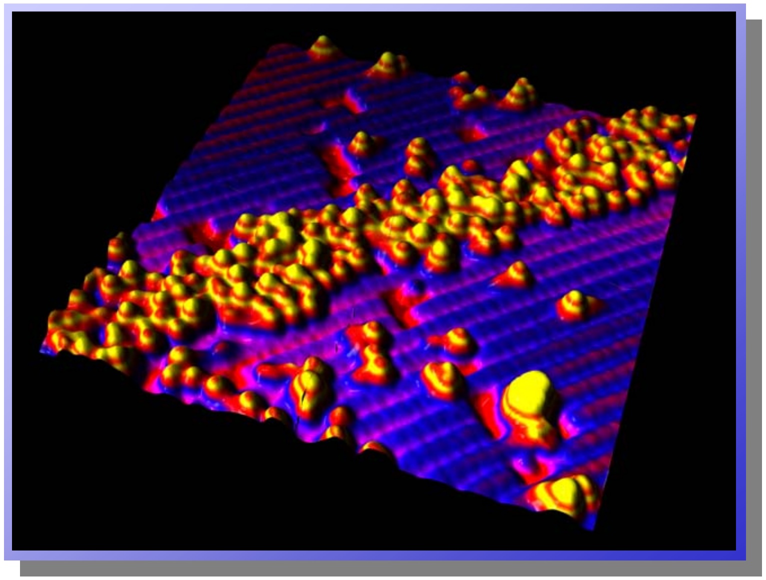

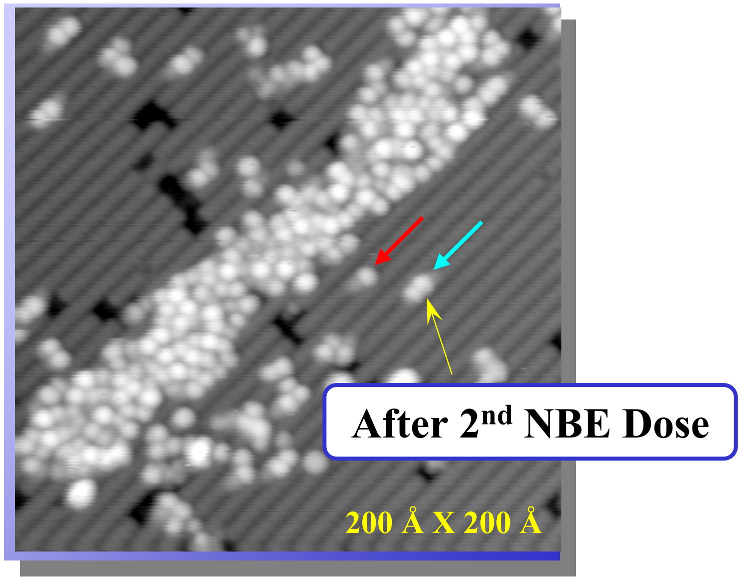

G. C. Abeln, *et al.*, *J. Vac. Sci. Technol. B*, **16**, 3874 (1998).

# Feedback Controlled Lithography

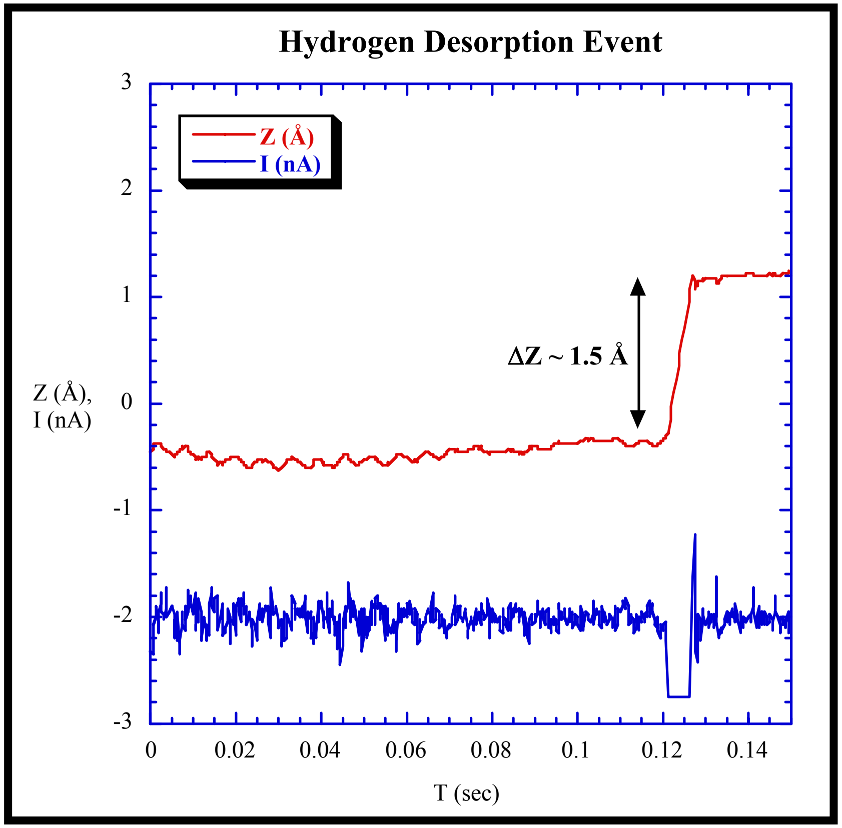

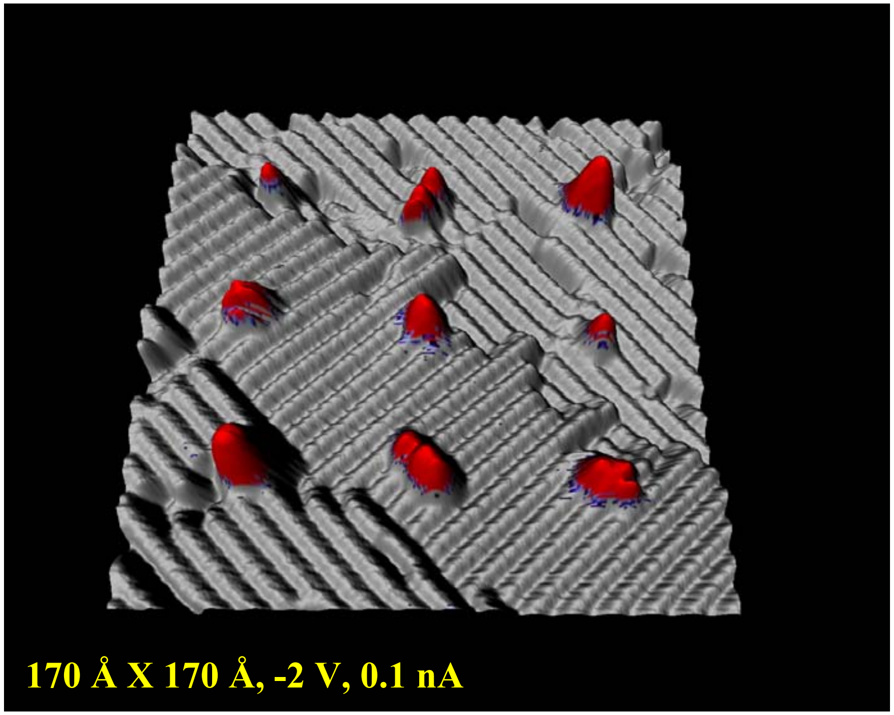

M. C. Hersam, *et al.*, *Nanotechnology*, **11**, 70 (2000).

# Self-Directed Growth of Styrene Chains from Individual Dangling Bonds

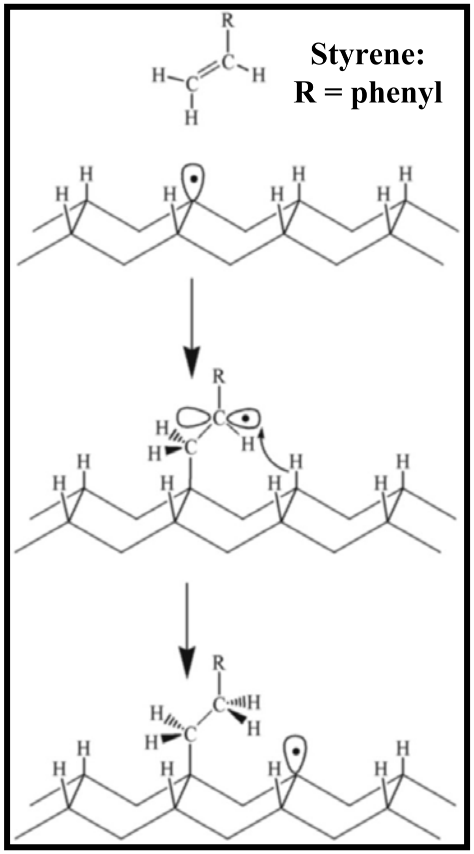

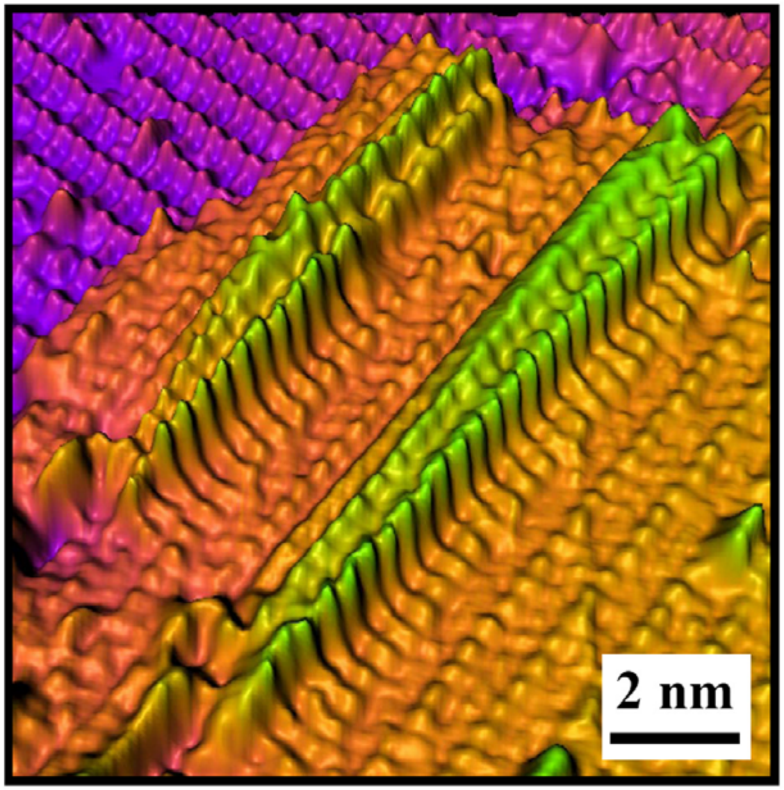

G.P Lopinski, *et al.*, *Nature*, **406**, 48 (2000).

# Heteromolecular Nanostructures via Multi-Step FCL

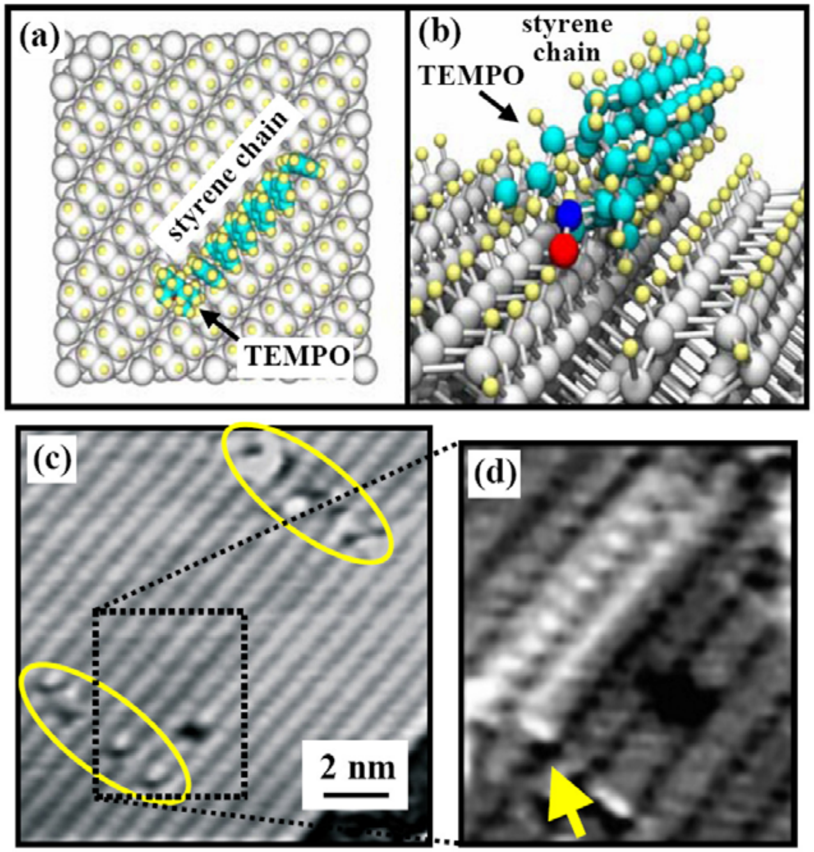

# Degenerately Doped Si(100) Surfaces

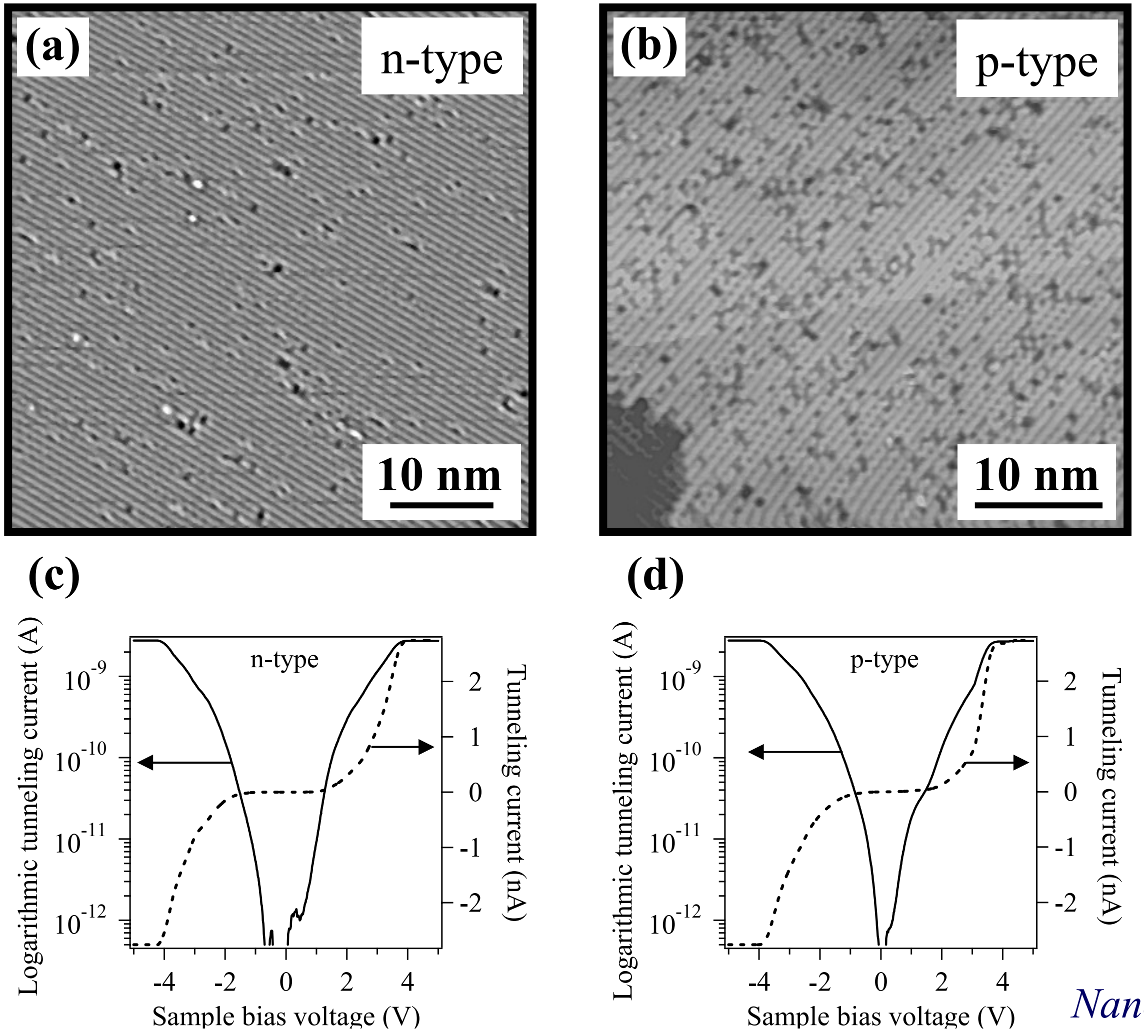

N. P. Guisinger, *et al.*,
*Nanotechology*, **15**, S452 (2004).

# TEMPO on the Si(100)-2×1 Surface

N. P. Guisinger, *et al.*, *Nano Lett.*, **4**, 55 (2004).

## TEMPO:
## (2,2,6,6-tetramethyl-1-piperidinyloxy)

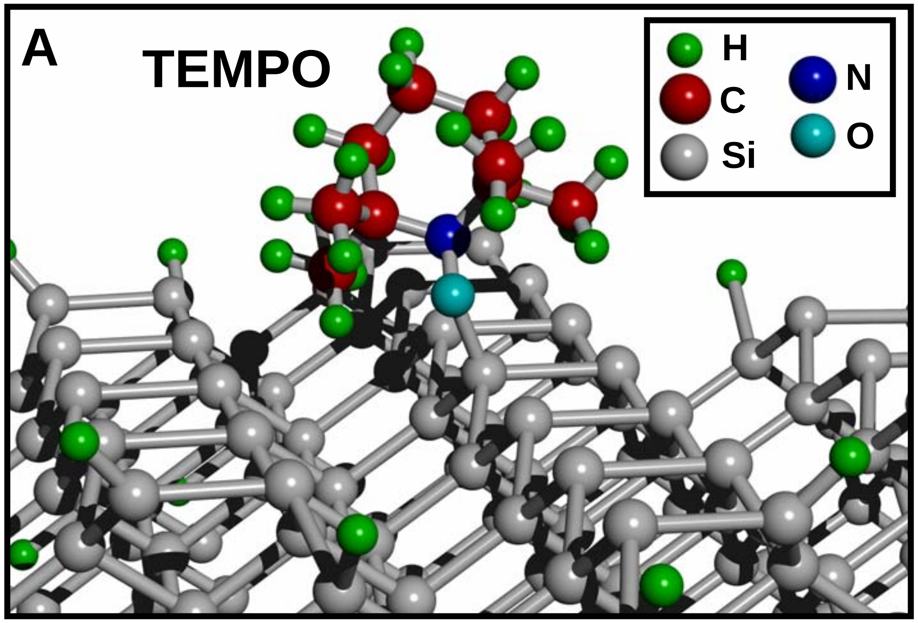

DFT Optimized Geometry (Hyper Chem Release 7)

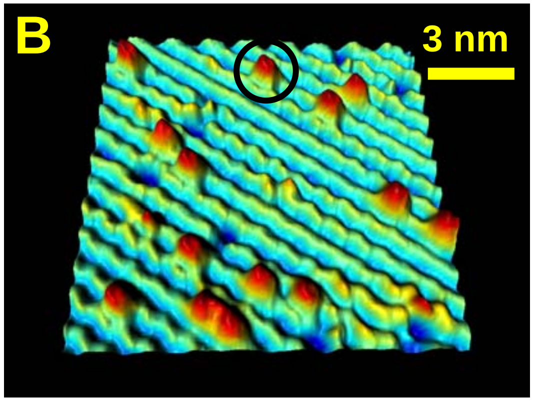

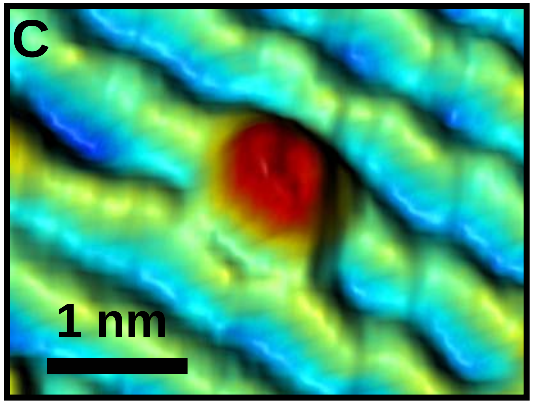

## Individual TEMPO molecules are probed with the STM

# I-V Curve for TEMPO on $n^+$-Si(100)

N. P. Guisinger, *et al.*, *Nano Lett.*, **4**, 55 (2004).

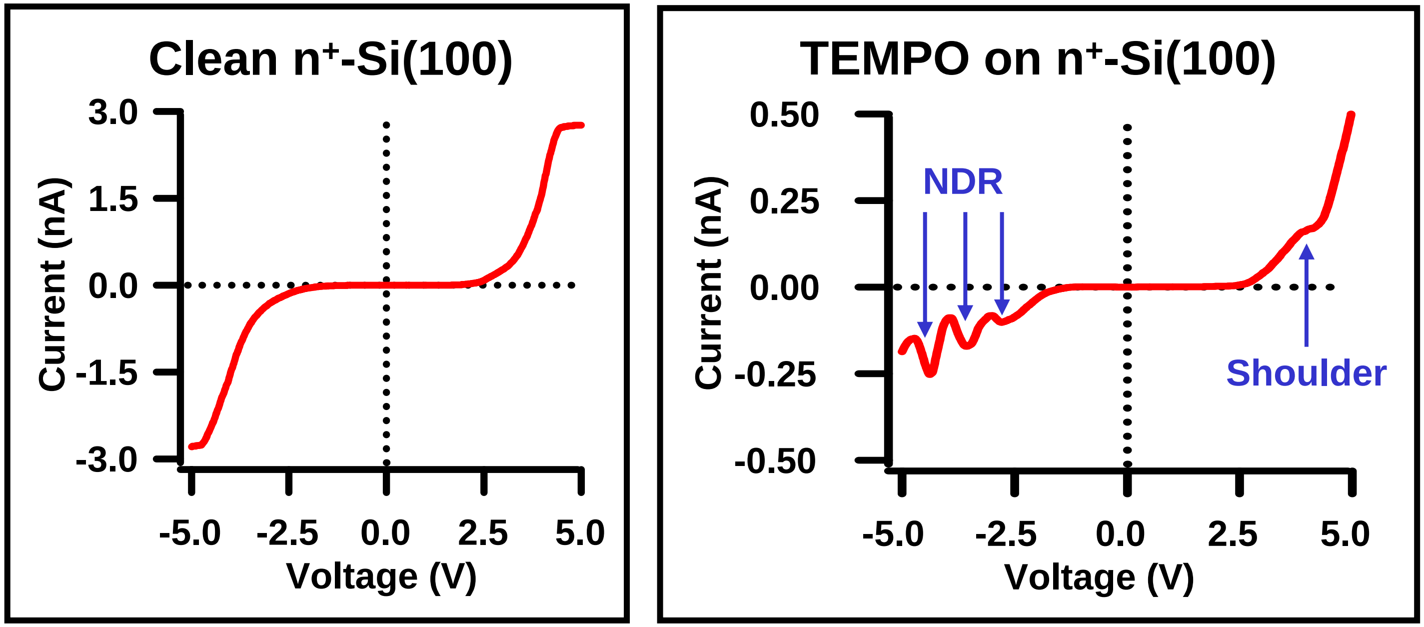

- NDR events are only observed at negative sample bias.
- Shoulder is only observed at positive sample bias.
- NDR bias values depend sensitively on tip-sample spacing
- NDR is observed in both bias sweep directions

# I-V Curve for TEMPO on $p^+$-Si(100)

N. P. Guisinger, *et al.*, *Nano Lett.*, **4**, 55 (2004).

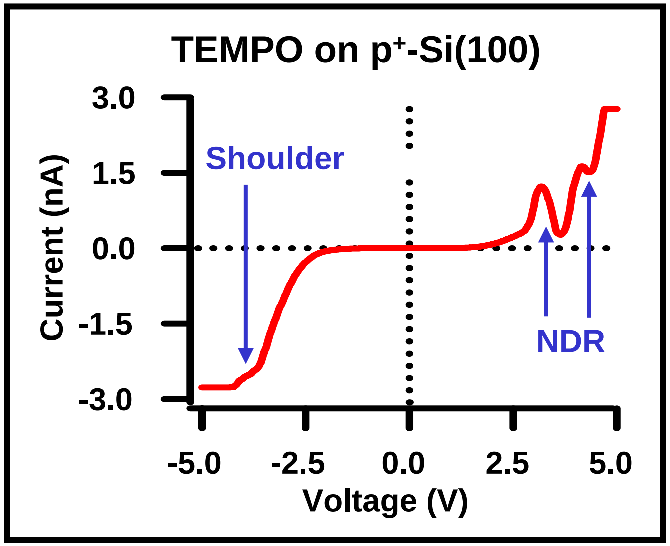

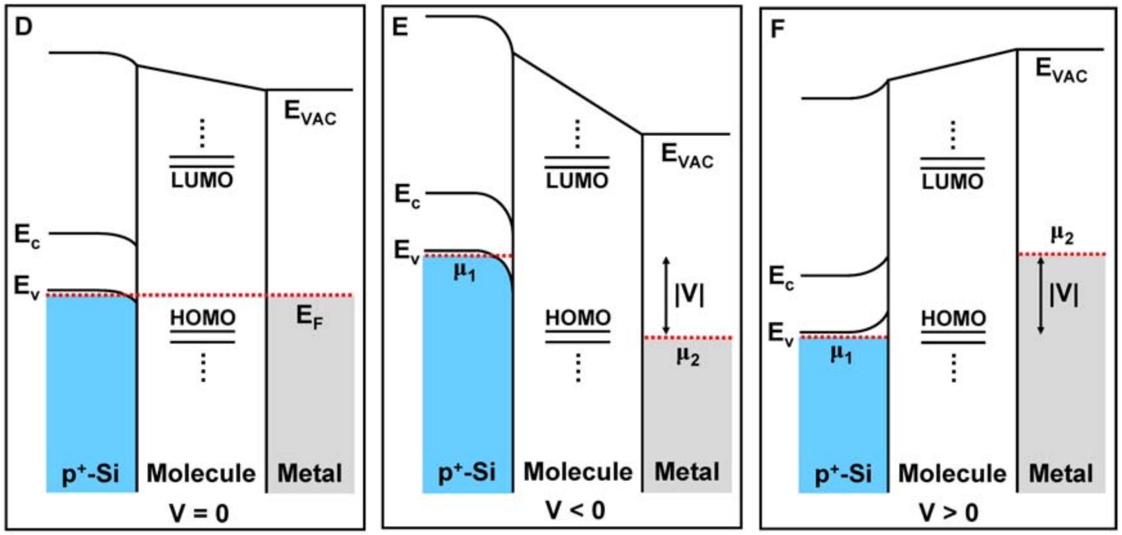

**Equilibrium** **Shoulder** **NDR**

- Qualitatively similar behavior to TEMPO on $n^+$-Si(100) except opposite polarity.
- Orbital energy shift may be due to charge transfer with the substrate.

# STM Spectroscopy: CuPc and Au Nanoelectrodes on NiAl(110)

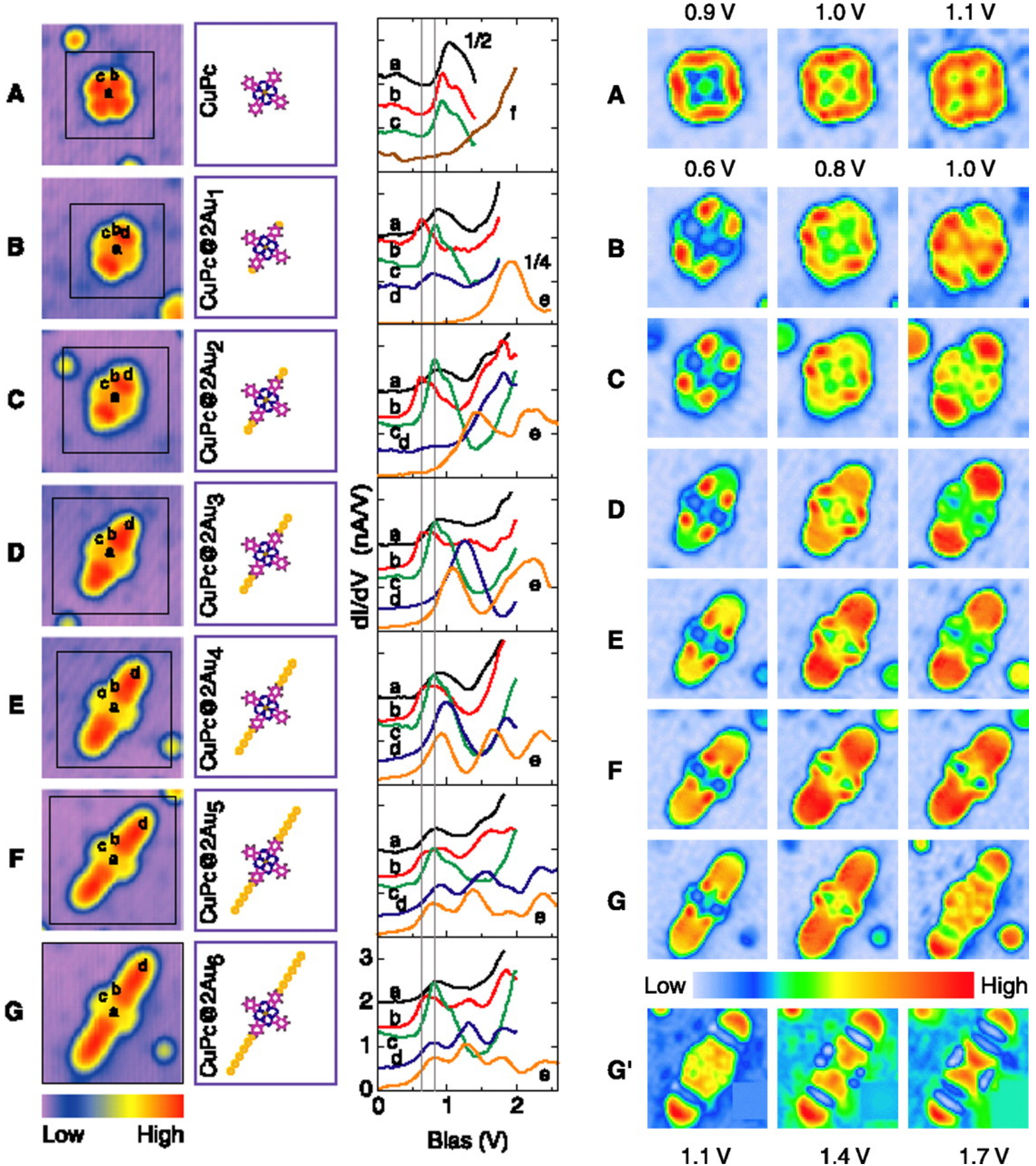

G. V. Nazin, *et al.*,
*Science*, **302**, 77 (2003).

# $C_2H_2$ on Cu(100)

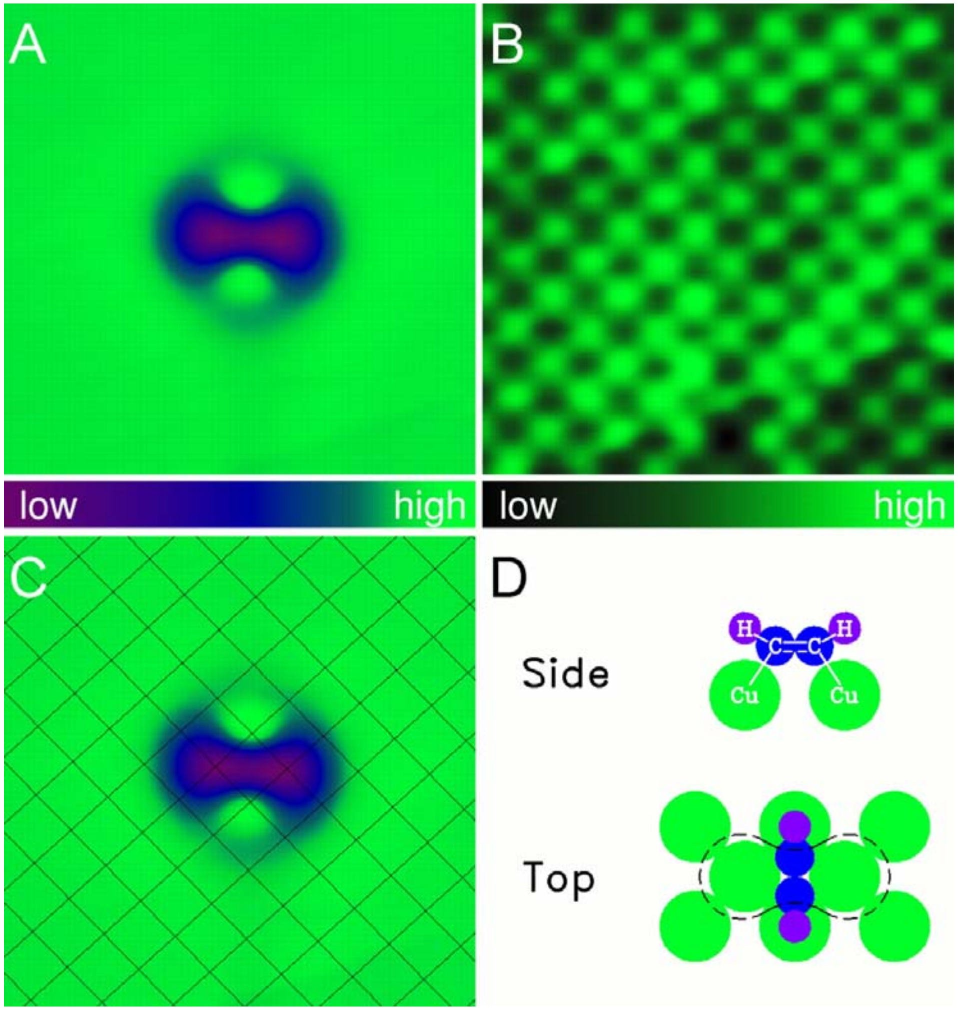

B. C. Stipe, *et al.*,
*Science*, **280**, 1732 (1998).

# Inelastic Electron Tunneling Spectroscopy

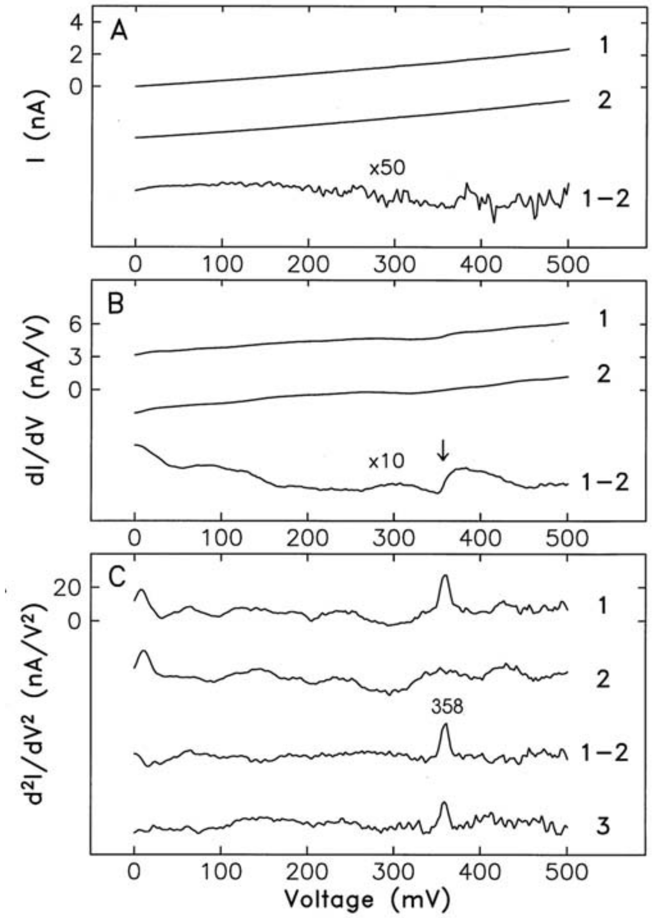

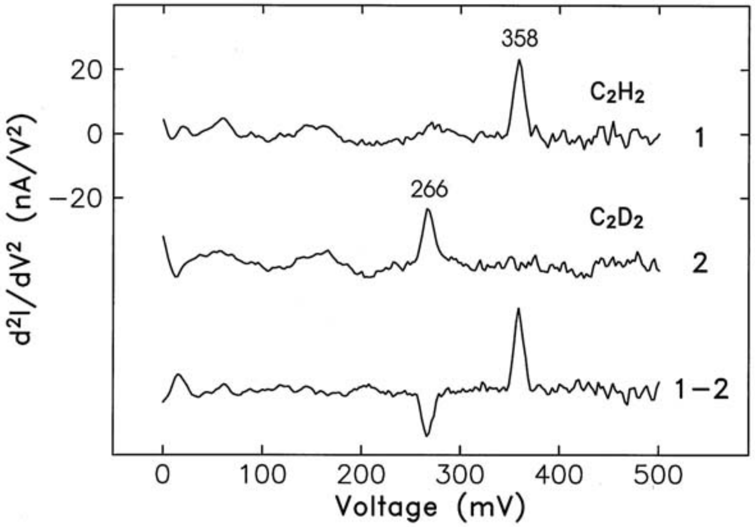

B. C. Stipe, *et al.*,
*Science*, **280**, 1732 (1998).

# Spatial Maps of $d^2I/dV^2$

Topo

$d^2I/dV^2$ @ 358 mV

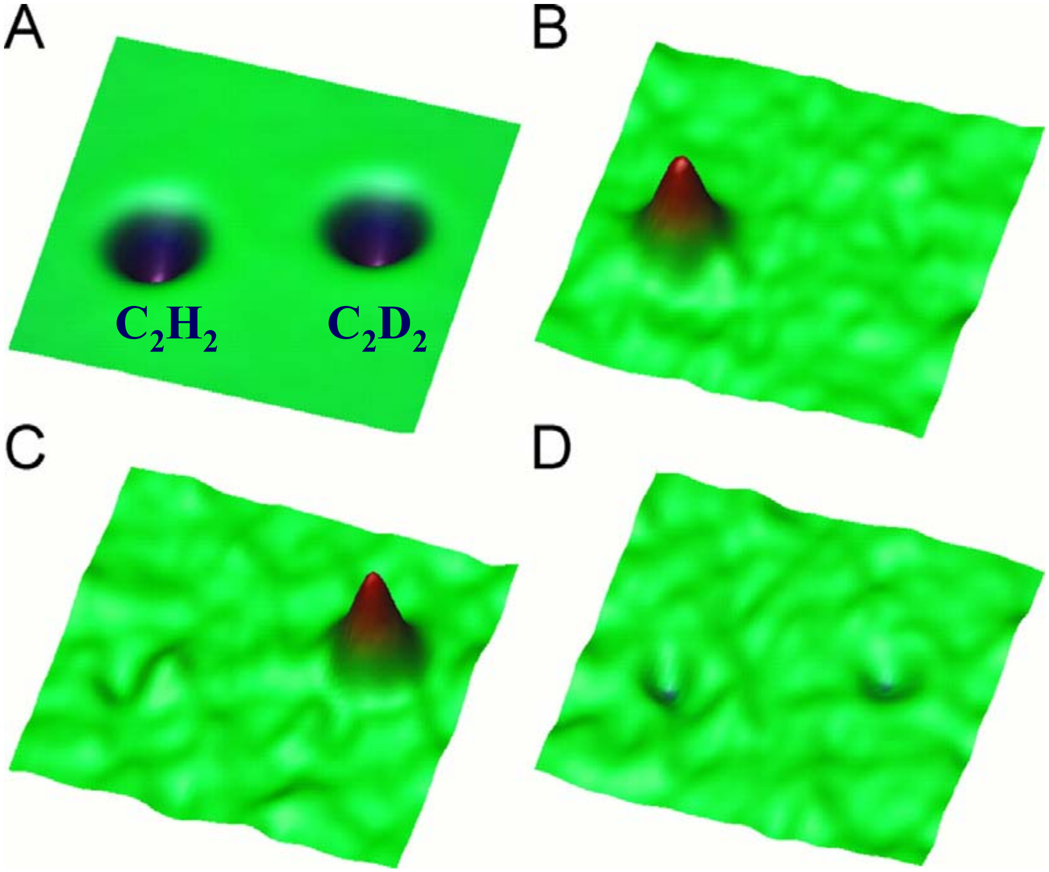

$d^2I/dV^2$ @ 266 mV

$d^2I/dV^2$ @ 311 mV

B. C. Stipe, *et al.*, *Science*, **280**, 1732 (1998).

# Contact Mode AFM Potentiometry

## Experimental setup:

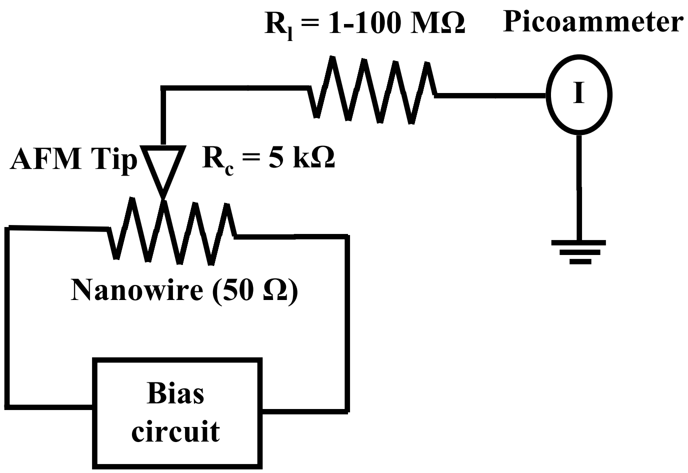

## Resolution requirements:

**To analyze nanowire failure,**

- Spatial resolution < 10 nm
- Voltage sensitivity < 100 µV

## Requirements of AFM tip:

- Conductive tip with small $R_c$ (kΩ range).
- Low $R_c$ must be sustained after extensive scanning in contact mode.

**Conductive diamond coated Si tips provide $R_c$ = 5 kΩ with low wear at a repulsive force of 0.54 µN.**

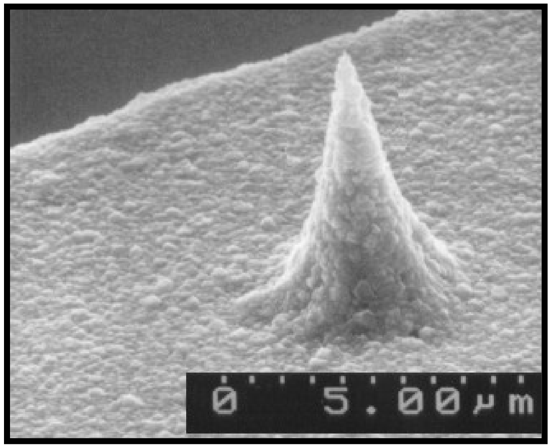

# Noncontact vs. Contact AFM Potentiometry

Noncontact mode:

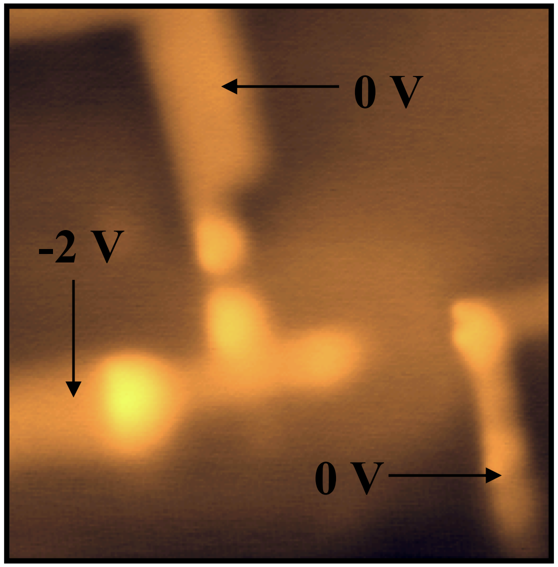

Image size = (1000 nm)$^2$

**Contact mode:**

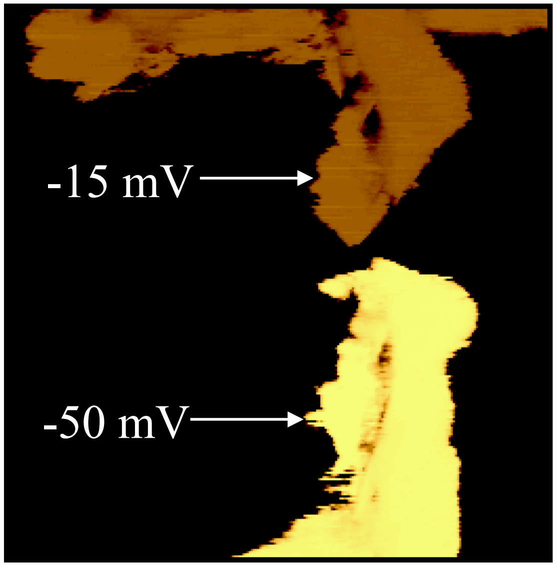

Image size = (500 nm)$^2$

**Contact mode:**

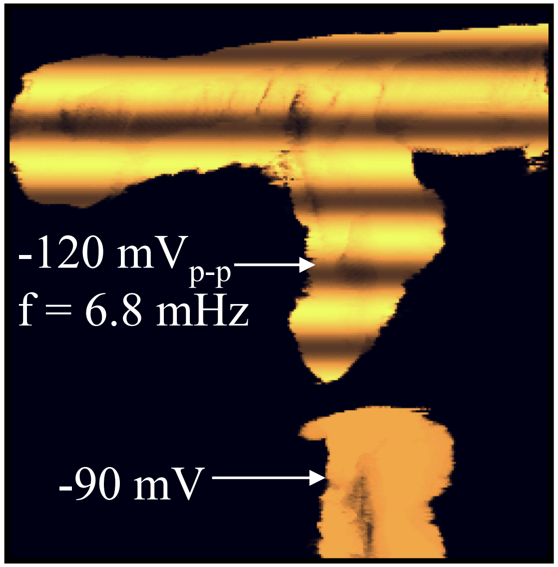

Image size = (500 nm)$^2$

- Noncontact mode AFM potentiometry possesses **~50 mV** potential sensitivity and **~50 nm** spatial resolution.
- Contact mode AFM potentiometry possesses **~1 µV** potential sensitivity, **~5 nm** spatial resolution, and **~0.01 ms** time response.

# AFM Potentiometry of Nanowire Failure

**Evolution of nanowire failure**:

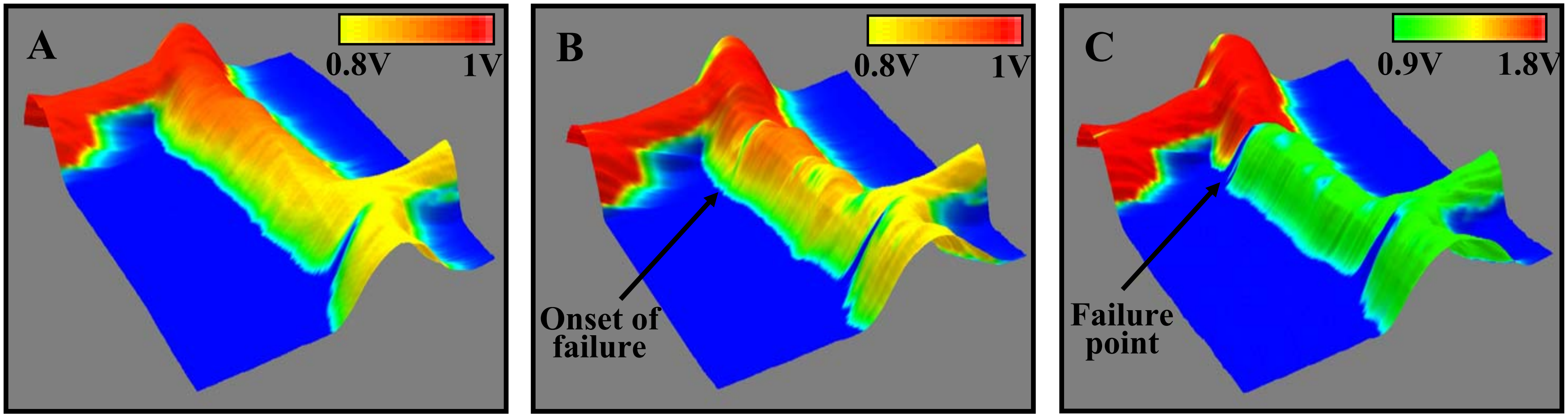

Contact mode AFM potentiometry images: Wire width = 60 nm

(Breakdown current density = $3.75\times10^{12}$ A/m$^2$).

M. C. Hersam, *et al.*, *Appl. Phys. Lett.*, **72**, 915 (1998).

# Atomic Force Electroluminescence Microscopy

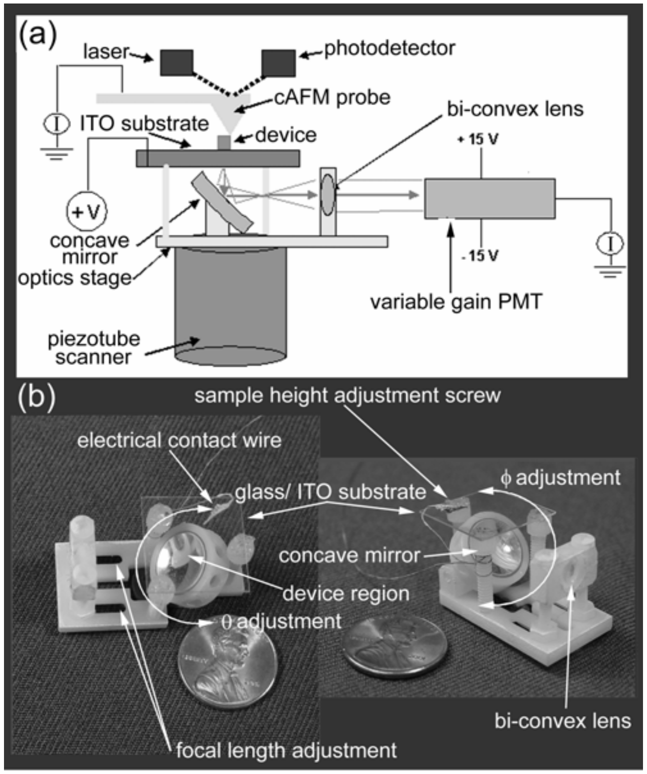

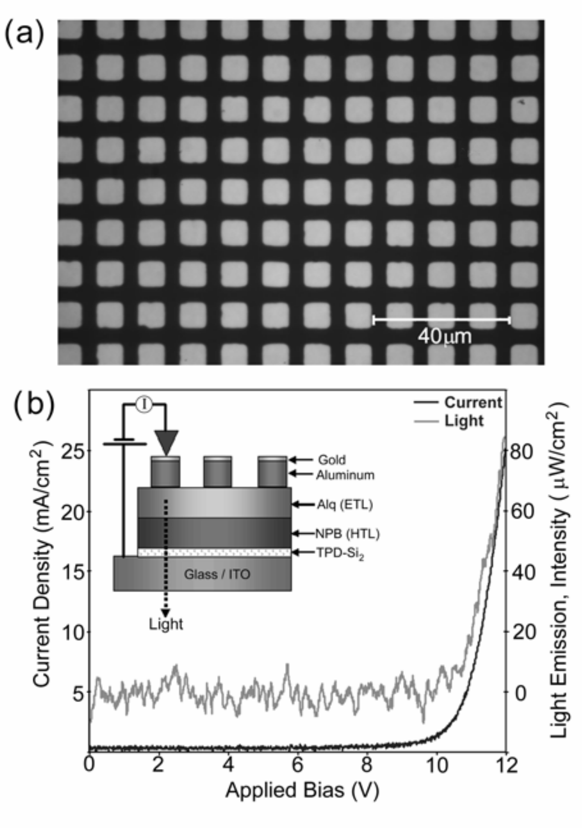

L. S. C. Pingree, *et al.*, *Appl. Phys. Lett.*, **85**, 344 (2004).

# AFEM on Micron Scale OLED Pixels

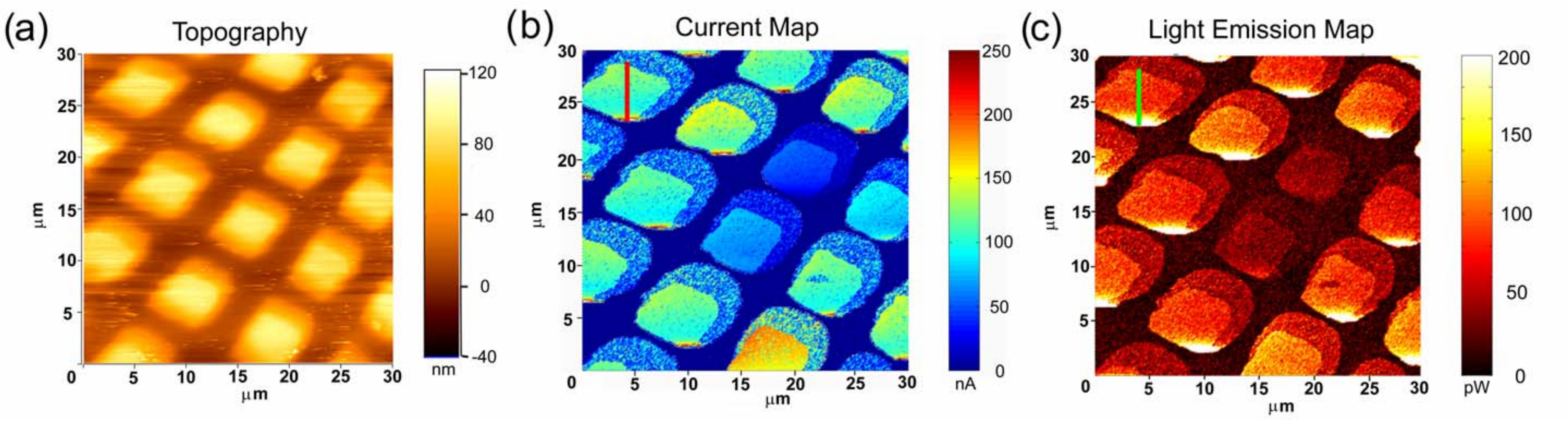

- Spatial and temporal variations in current flow and electroluminescence can be directly probed.

L. S. C. Pingree, *et al.*, *Appl. Phys. Lett.*, **85**, 344 (2004).